NHSH CR-176,968

NASA-CR-176968
19860019444

A Reproduced Copy

OF

N86-28916

Reproduced for NASA

by the

NASA Scientific and Technical Information Facility

NF01694

FFNo 672 Aug 65

THE USE OF A PANEL CODE ON HIGH LIFT

CONFIGURATIONS OF A SWEPT

FORWARD WING

FINAL REPORT

PRINCIPAL INVESTIGATORS

James Scott Scheib

Doral R. Sandlin

09/31/83 - 03/31/85

California Polytechnic State University

Aeronautical Engineering Department

San Luis Obispo, California

Grant No. NCC2-255

ABSTRACT

THE USE OF A PANEL CODE ON HIGH LIFT

CONFIGURATIONS OF A

SWEPT FORWARD WING

James Scott Scheib

February 1986

As part of a research project at the NASA Ames Research
Center, a study was done on high lift configurations of a
generic swept forward wing using a panel code prediction
method. A survey was done of existing codes available at
Ames, from which the program VSAERO was chosen. The
results of VSAERO were compared with data obtained, when
available, from the Ames 7- by 10-foot wind tunnel. The
results of the comparison in lift were good (within 3.5%).
The comparison of the pressure coefficients was also good.
The pitching moment coefficients obtained by VSAERO were
not in good agreement with experiment. This might be
traced to VSAERO's tendency to overpredict the suction peak
due to the sharp leading edge. VSAERO's ability to predict
drag is questionable and cannot be counted on for accurate
trends. Further studies were done on the effects of a
leading edge glove, canards, leading edge sweeps and
various wing twists on spanwise loading and trim lift with

ii

encouraging results. An unsuccessful attempt was made to model spanwise blowing and boundary layer control on the trailing edge flap. The potential results of VSAERO were compared with experimental data of flap deflections with boundary layer control to check the first order effects. The experimentally determined CLs with boundary layer control were higher than VSAERO, possibly due to jet flap effects.

Table of Contents

List of Tables

List of Figures

List of Symbols

CL	Lift coefficient
Cl	local Lift Coefficient
CD	Drag Coefficient
CM	Pitching Moment Coefficient
CP	Pressure Coefficient
psf	pounds per square foot
fps	feet per second
Qmax	maximum dynamic pressure in 7- by 10-foot wind tunnel test
$C\mu$	Blowing Coefficient for spanwise blowing and boundary layer control
α	angle of attack
MAC	Mean Aerodynamic Chord
X/C	Percent Chord
$\frac{2y}{b}$	Percent Semispan
c	Local Chord
$\bar{c}$	Average Chord

CHAPTER 1

Introduction

In recent years, interest in swept forward wings (SFW) has developed due to advances in aeroelastic tayloring of composite structures. With the problem of aeroelastic divergence solved, the SFW is now a viable alternative to the conventional aft swept wing aircraft. Many advantages are hoped to be gained by using this configuration. Among them are lower trim drag at subsonic speeds, better low-speed handling, higher volumetric efficiencies and lower wave drag. Recent studies of the high speed characteristics of swept forward wings have verified that trimmed lift/drag ratios of aircraft having SFW configurations can surpass those currently obtainable using aft swept wings A flight test program has been started by the Defense Advanced Research Projects Agency (DARPA) with Grummann to investigate flight handling qualities of an aircraft, the X-29, configured with a swept forward wing.

As part of a long-range research effort in applications of powered lift, Ames Research Center is investigating the application of powered lift devices to a generic swept forward wing configuration. Large and small wind tunnel tests will be made on the configuration, to not only evaluate the effectiveness of the powered lift devices used, but also to establish well-documented experimental

data that can serve as verification for aerodynamic predic-
tion techniques which are now under development. As part
of this effort, panel codes are being used which are suffi-
ciently computer efficient to allow the user to look at
many configurations of a particular propulsion lift con-
cept. The panel codes provide information on what aspects
of the configuration show the most promise and are, there-
fore, most desirable to investigate further experimentally
as well as theoretically. This investigation utilizes one
of these prediction techniques, VSAERO, in the study of
aerodynamic parameters, CL, CD, CM and CP in high lift con-
figurations applied to the SFW. The project also included
an evaluation of the applicability of the technique itself.

CHAPTER 2

Procedure

Choice of Prediction Technique

Use of panel codes in preliminary design is rapidly developing. Their accuracy in predicting potential results is good. However, improvement is still needed in modeling viscous effects, wake interference, jet effects and flow separation. The programs available are currently extending their applications to powered lift and becoming more user oriented.

The first task of the project was to choose from some of the panel code programs available in industry. The codes considered for this choice had features which, for some problems, could simulate viscous and power effects. These include VSAERO, written by Analytical Methods Incorporated (AMI); PAN AIR, developed by Boeing and modified by General Dynamics; MCAERO, developed by McDonnell Douglas; and the Vought VAPE program. These codes were studied for applicability to the current study, evaluating SFW aerodynamics of aircraft concepts operating at low speed with high lift. They should also be able to incorporate canard and lifting device effects, as well as spanwise blowing and boundary layer control on the flaps. Additional features of utility and economy are also important.

3

The cores of the programs are 3-D inviced panel methods. All have first order viscous/power effects modeling options such as the integral models of boundary layers or jets in cross flow. They use source and doublet distributions to model the flow over arbitrary shapes. The way in which these flow properties are distributed makes each program unique.

PAN AIR is a higher order panel method which uses a piecewise constant source distribution and a quadratically varying doublet distribution. The term "higher order" means that the panels in the PAN AIR code are broken down into subpanels. These subpanels make it possible to match the edges of the neighboring panels with a higher degree of accuracy. Matching the panel edges turns out to be very important when using a quadratically varying doublet distribution. Any leaks between the panels cause the doublet and source strengths to become numerically unstable.

MCAERO, VSAERO, and VAPE might all be considered lower order panel methods which require considerably less computing time. The difference between lower and higher order is slightly obscured with VAPE and MCAERO. MCAERO uses a constant source and a quadratic doublet distribution. VAPE simulates the flow with a uniform sink and doublet distribution. VSAERO uses a piecewise constant source and doublet distribution.

The programs also differ in which code they use in their 3-D potential calculations, what boundary layer

theory is incorporated, and what wake and jet models are used. See Table 1 for a breakdown of the methods.

Table 1

Panel Code Programs Overview

	VSAERO	PAN AIR	MCAERO	VAPE
Panel Method	L.O	H.O. Halsey Hess	L.O. MCAIR Surface P.M.	L.O. Hess
Source Doublet Distributions	Piecewise Source & Dblt	Piece Source Quad Dblt	Const Source Quad Dblt	Uniform Sink & Dblt
3-D Potential		Prandil-Gluaret	Bristow Hawk	Whooler
Boundary Layer	Integral Source Trans	Integral Whitefield	Integral	Finite Diff. Strip
JET MODEL	FEARN WESTON	RAXJET	ADLER BAPON	WHOOLER WESTON AND THAMES
Wake	Iter Relax Jet Wake	User Spec Jet Wake	Jet Wake Only	Jet Wake Only

After careful consideration, VSAERO was chosen over the other three programs. The first two programs, VAPE and MCAERO, were eliminated in part by their lack of availability at the time. Neither of these programs were working with any reliability on any of the NASA computers

accessible at the start of this project. The remaining two
programs were the more established of the four, and were
considered as the two main choices initially.

VSAERO vs. PAN AIR

When choosing VSAERO, one of the considerations was
VSAERO's availability. There was a 1000 panel version
operational on both the 40- by 80- wind tunnel's local VAX
computer and the NODE FHW on NASA's central computer sys-
tem. Two versions of VSAERO were on NASA's Cray X-MP
computer, a 1000 panel and a 3000 panel version. Because
PAN AIR requires more computer space than the VAX computers
have available, its code was limited to the more expensive
Cray computer. In general, PAN AIR was significantly more
expensive per run than VSAERO. In the opinion of the
author, it is not as important to have a higher order panel
method when running subsonically as it is for the super-
sonic case. PAN AIR was designed to handle both the
subsonic and supersonic case, whereas VSAERO was designed
primarily for subsonic high lift applications and is con-
sidered as reliable as PAN AIR in that flight regime.

Another major factor in the decision to use VSAERO was
the fact that, at the time available for use, it had a wake
relaxation routine. PAN AIR, which had only a user defined
wake, was in the process of developing a similar feature
for future use. On the SFW model, canard wakes play an
important role in the wing's overall lift distribution and
stall characteristics. The wake relaxation routine

accounts for canard wake interference effects. Cases run
on VSAERO ran wakes off the trailing edges of the wing and
canard to model an unseparated flow, or ideal case. For a
separated flow, VSAERO has an option to specify a separated
wake which can be paneled on the wing along the separation
line.

A third factor in choosing VSAERO was the range in
configurations which could be run with simple changes in
the input file. VSAERO has many features which allow the
user to quickly change the geometry of the panels. PAN AIR
requires all corner points of all panels to be defined by
the user. General Dynamics has written a preprocessor
module to help the user create the large data file required
by PAN AIR. For each different configuration, a separate
run through the preprocessor is still required. VSAERO
will generate most of the geometry using its internal
geometry routing. The geometry of any VSAERO file can be
easily checked by setting the input variable MSTOP to two
or three. This will terminate execution after generating a
plot file of the geometry or the geometry plus wake. This
cuts the computing time during the initial configuration
layout to a few minutes per run on the VAX. The plotting
routine, PLTVSA, also developed by AMI, is used to get a
picture of the configuration using one of the output files
generated by VSAERO. This made VSAERO a more user friendly
program for this application.

The capability to handle thrusting jets such as span-
wise blowing and boundary layer control (BLC) on the flaps
was another consideration studied. The method attempted in
modeling BLC and blowing would be to use the jet wake
capabilities in PAN AIR, or the jet modeling or normal
velocity options in VSAERO. Although there has been some
preliminary evaluation of this modeling by the developing
companies, it was not known which program would model the
SFW powered lift devices with more accuracy, or if either
could model the situation at all. None of the programs
available had ever been used for this application. The jet
wake routines included in these panel codes are designed
for a jet in cross flow and do not allow for interaction
between the lifting surface and the jet wake.

From the foregoing considerations of the relative ease
of use and computer efficiency, as well as relative
treatment in modeling power and viscous effects, VSAERO was
thought to provide the best chance for success in this type
of application.

VSAERO

VSAERO, developed by AMI, is a program used for calcu-
lating the nonlinear aerodynamic characteristics of
arbitrary configurations in subsonic flow. VSAERO uses a
surface singularity panel method with quadrilateral panels
and piecewise constant source and doublet singularities.
Sources are solved directly from the external Neumann
boundary condition solving the normal component of the

flow. Doublet values are solved by imposing the internal Dirichlet boundary condition of zero perturbation potential at the centers of all the panels simultaneously; the gradient of the doublet distribution is used to obtain the surface perturbations velocities. An iterative wake shape calculation procedure models the effects of vortex separation and vortex/surface interaction. An iterative loop, coupling potential flow and an integral boundary layer calculation, treats the effect of viscosity.

The program is designed for high lift configurations of complete aircraft, including wings, bodies, tailplanes, fins, slats, slotted flaps, powered nacelles, etc. It can be run in a symmetric or asymmetric configuration along the X-Y plane. A simulated ground plane can be defined along the X-Z plane at Y equal to zero. Nonzero normal velocities can be specified for inflow or outflow from specially defined panels. Vortex sheet wakes representing the shear between the jet and local velocities can be attached to represent powered nacelles. Surface and off body streamlines and velocity surveys can be requested. Two integral boundary layer calculation options are provided in a viscous/potential iteration coupling. The program generates a plot file of the geometry and aerodynamic data as well as an output file of the data.

Configurations Studied

The choice of the wing to be modeled was based on the
wind tunnel test configuration in the NASA Ames 7- by 10-
foot wind tunnel of the SFW semispan model. The complete
layout of the test is shown in Figures 1 and 2. It was
hoped that this test would provide a good data base for the
project. The symmetric airfoil has a 5% thickness-to-chord
ratio, with a 30° negative leading edge sweep. See Table 2
for the wing geometry. Spanwise blowing and BLC flaps were
incorporated in the model. The model has both leading and
trailing edge flaps on the main wing, as well as an
optional leading edge glove. The capabilities of the model
are listed in Table 3.

The two canards for the wind tunnel model were also
used in this project, although wind tunnel data is not yet
available for wing and canard configurations. Canard 1 is
41% of the wing area, while Canard 2 is 30% of the wing
area. Both canards have a 45° leading edge sweep and a
symmetric 4% thickness airfoil. They are also able to be
deflected up to 30° with respect to the wing, and moved to
three longitudinal positions. For canard specifications,
see Tables 4 and 5.

The wind tunnel test was run at a dynamic pressure of
25 PSF, which corresponds to a velocity of 145 fps
(Mach 0.13). All configurations were run at angles of
attack from -5° to 45°. The wind tunnel test ran
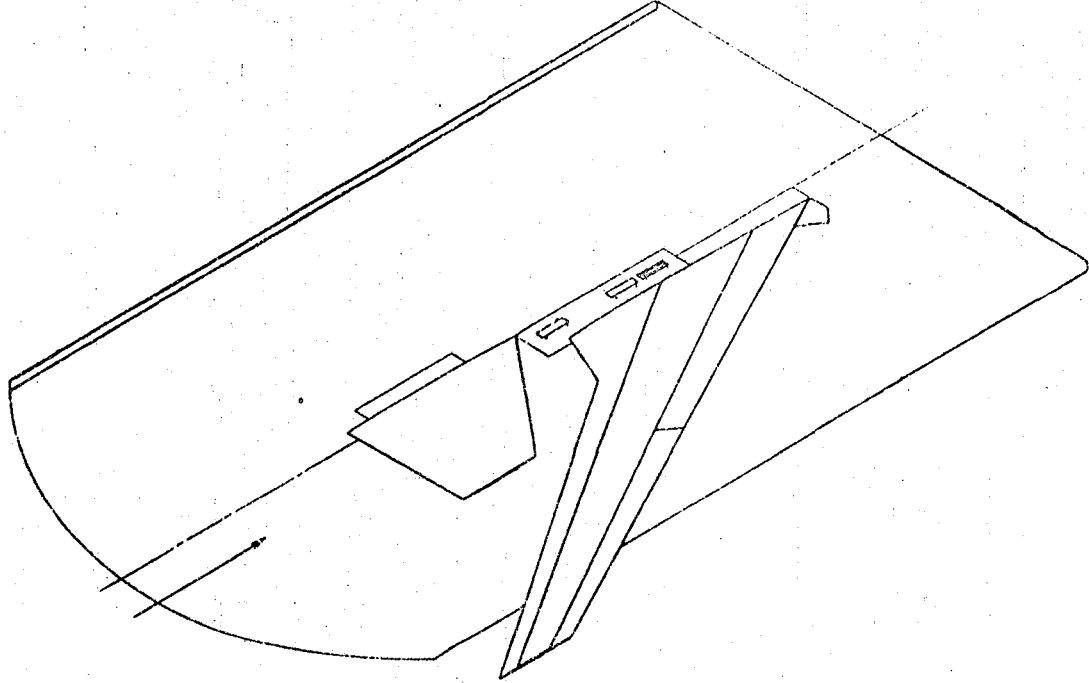cases of wing alone and wing/glove combinations.

Figure 1

Seven- by Ten-Foot Wind Tunnel Model Layout

Figure 2

Seven- by Ten-Foot Wind Tunnel Model Layout

Table 2

Swept Forward Wing Specifications

Area (exposed)	706.98 sq. in.
Semispan	35.67 in.
L.E. sweep	-30°
T.E. sweep	-43.8°
Aspect ratio	3.6
Taper ratio	0.49
Root chord	26.64 in.
Tip chord	13.00 in.
Mean aerodynamic chord	20.61 in.
Dihedral	0°
Twist	0°
Airfoil section	64A005

Table 3

Seven- by Ten-Foot Swept Forward Wing
Model Capabilities

Q_{max}	30 psf
Angle of attack range	$-15° < \quad < 45°$
Trailing edge flap deflections	15°, 30°, 45°
Leading edge flap deflections	15°, 30°
Canard deflections	0, ±5°, ±15°, ±30°
Spanwise blowing angles	0, -30°, -40°
Spanwise blowing location	3 positions (see Fig. 1)
Canard location	3 positions
Leading edge glove	on/off
Canard configuration	Canard 1, Canard 2, no canard

Table 4

Canard 1 Geometry Specifications

Area	290.28 sq. in.
Span	17.01 in.
L.E. sweep	45°
T.E. sweep	10.7°
Root chord	24.00 in.
Tip chord	10.13 in.
Aspect ratio	2.0
Taper ratio	.42
Dihedral	3°
Twist	0°
Airfoil section	64A004
Mean aerodynamic chord	17.96 in.

Table 5

Canard 2 Geometry Specifications

Area	210.52 sq. in.
Span	12.13 in.
L.E. sweep	45°
T.E. sweep	−35°
Root chord	27.67 in.
Tip chord	7.04 in.
Aspect ratio	1.4
Taper ratio	.25
Dihedral	3°
Twist	0°
Airfoil section	64A004
Mean aerodynamic chord	19.41 in.

Configurations studied were those of various combinations
of flap settings, boundary layer control on the trailing
edge flap, and spanwise blowing. The model will be
rescheduled to run in a 7- by 10-foot wind tunnel so the
full range of its capabilities can be tested, including
testing with the canards and split flap configurations.

Once the experimental results were compared to the
theoretical results of VSAERO, continued studies were done
to look at the effect of wing twists and different sweeps
on the spanwise loading and trim lift. The effect of the
canards and canard location was also considered when
examining spanwise loading and trim lift.

Since VSAERO gives a solution for potential flow with
only moderate allowance for boundary layer flow separation
effects, VSAERO calculations were thought to be a good
measure of expected performance of a wing at low angles of
attack with BLC on the trailing edge flap. It should be
stressed that at the time of this investigation there was a
concentrated effort underway by NASA to update VSAERO in
order to more accurately simulate effects of flow separa-
tion and to model power-induced aerodynamic
characteristics. Because of the experimental nature of the
available code changes, it was decided not to use them for
this project.

An attempt to model the first order effects of span-
wise blowing and BLC were also made using an angle of
attack of 5° and a trailing edge flap deflection of 30°.

During this phase of the investigation, the output of VSAERO was matched to experimental results to find the best representation of the power induced effects.

Paneling the Swept Forward Wing

The basic swept forward wing was first paneled in the clean configuration. Node points were placed at the 20% and 70% chord positions which locate the leading and trailing edge flap positions. These nodes can be used to rotate the flaps about the unit normal vector, which is along the flap hinge line. See Figure 3 for node card placement on wing geometry. Although VSAERO will bend the flap for the user, it was thought better to define the flaps manually due to VSAERO's tendency to deform the wing. The coordinates of the flap settings were calculated using a short program. Seven different files were created, which included the four trailing edge flap settings and the three leading edge flap positions. A final file was created of the leading edge glove coordinates, which were input onto the original file to model the wing/glove configuration. These coordinates could be arranged into any configuration desired.

The main wing's axis origin was placed at the leading edge of the root chord, which was also the origin of the global coordinate system. With VSAERO, positive X is streamwise and positive Z is vertical. All moments were taken about X location of the quarter chord position of the mean aerodynamic chord.
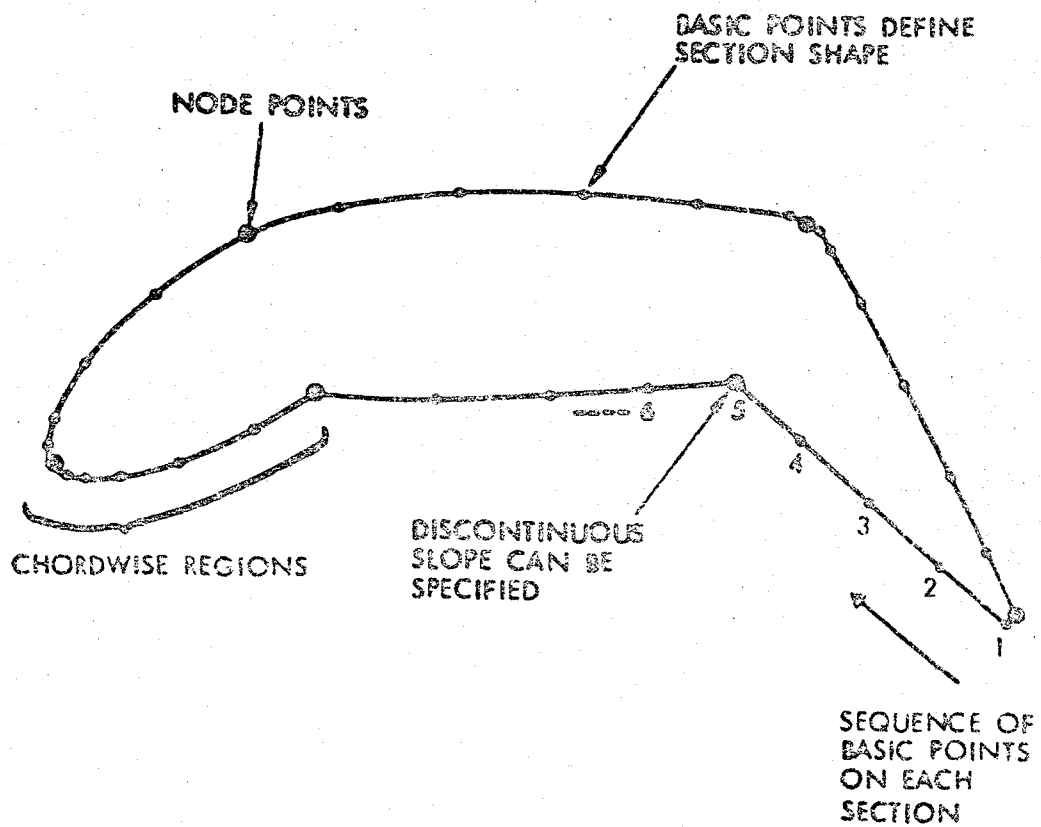
Figure 3

Node Card Placement of Swept Forward
Wing Section

Data points for both canards were then input, and copied onto the original file to create three main files. These include wing alone, wing plus canard one, and wing plus canard two. For a paneled representation of the three configurations with wake roll up, see Figures 4, 5, and 6. The canards were made separate components, with the origins of the component axes at what would be the pivot point of the canard on the semispan model. With this setup, the canards can be scaled, rotated and moved with respect to their own axes, as well as the main wing's axes.

A situation which could not be studied was the canard wake interference effect when the canard was at a high angle of attack. In these positions the canard wake passed directly through the main wing. This condition is not accepted by VSAERO and the solution diverges. To avoid this, the wake was defined to pass under the wing and then relaxed. When the wake was relaxed it again moved into the main wing and the solution diverged. The same situation arose when the wake was defined to flow over the wing. Because of this, the canards were limited to an angle of attack of 5° with respect to the main wing.

When deflecting the trailing edge flap at angles up to 45°, a method to model the separation was needed. The use of VSAERO has many options in defining a separated wake. The three main types of wakes are a regular wake, a separated wake, and a jet wake. All three can be fixed or relaxed using the iterative wake relaxing routine. How
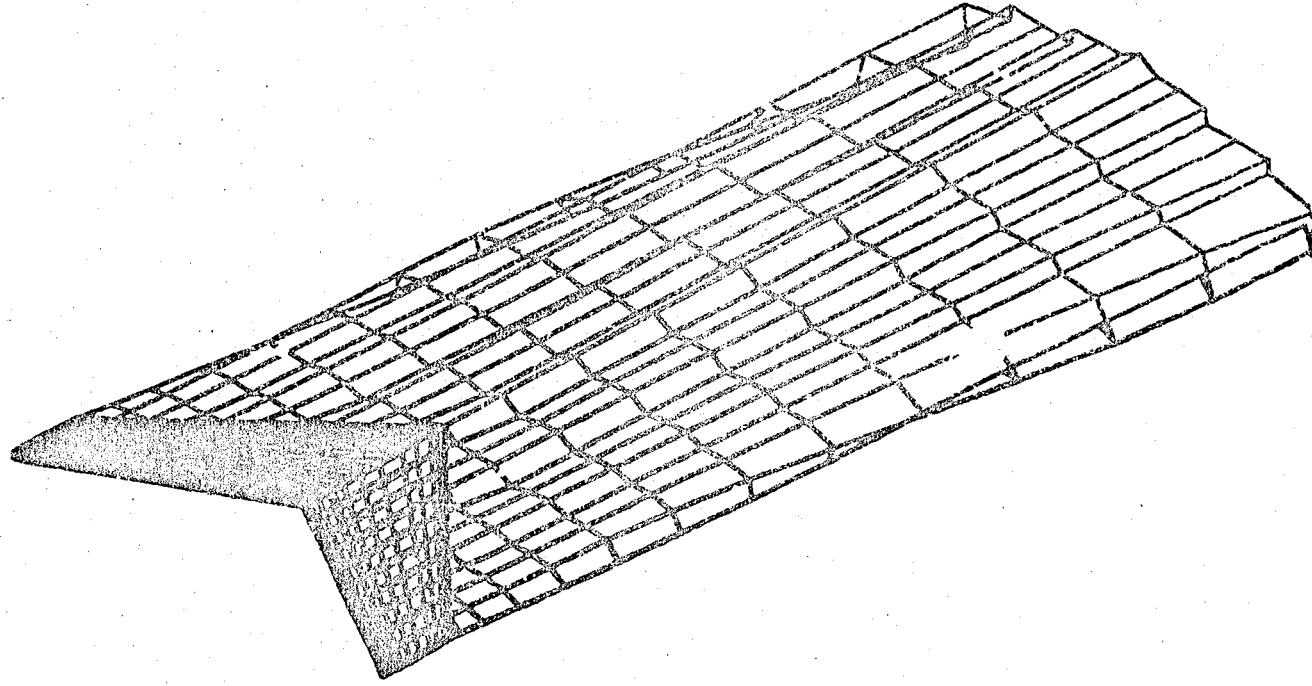
Figure 4

Paneled Representation of Wing With Wake
Roll Up at 5° α

Figure 5
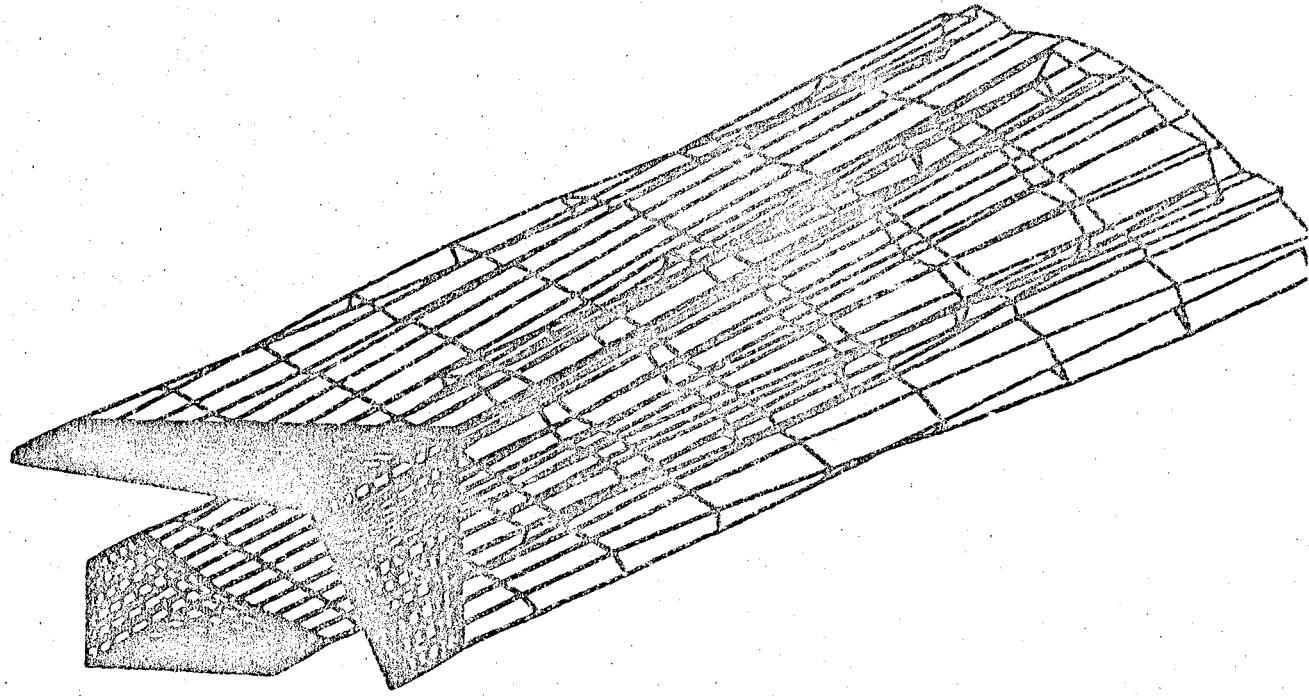
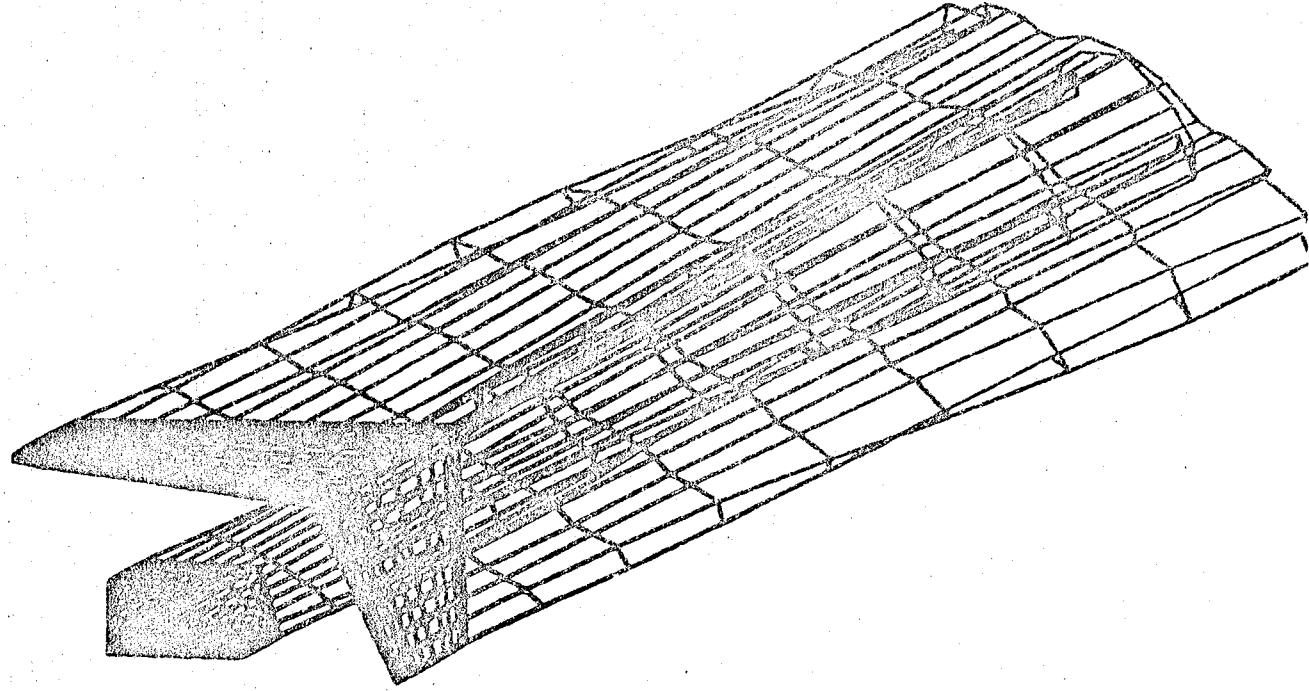Paneled Representation of Wing Plus Canard 1
With Wake Roll Up at 5° α

Figure 6

Paneled Representation of Wing Plus Canard 2
With Wake Roll Up at 5° α

these wakes are paneled on to the wing is also very important to the final results. A study was made of these various options in the hope of finding the best method of paneling this situation. See Appendix A for an explanation of how the best combination of wake and wake pattern was chosen.

Because VSAERO is a 3-D potential flow program, at an angle of attack greater than 15° the viscous iteration capabilities of the program were to be employed in modeling the boundary layer build-up and separation. However, with such a thin wing and sharp leading edge, VSAERO will calculate very high pressure coefficients at the leading edge, or suction peak. This will cause the boundary layer module to assume the wing has separation almost immediately with no turbulent reattachment. Once the boundary layer routine predicts separation, the displacement thickness is assumed constant for the remainder of the path down stream. Because this is not an accurate representation of the boundary layer, all viscous data is questionable. For this reason, no viscous iterations were run.

It should be noted that this is a problem of all panel methods unless a more accurate flow model of the separated flow regime is available. Three dimensional potential programs in general will give the same high pressure coefficients at the leading edge. Without the use of the viscous iteration option, it was not possible to obtain any data on when separation may occur or where the separation

line exists.   VSAERO also cannot model the advent of a

leading edge vortex which occurs at higher angles of

attack.

CHAPTER 3

Discussion and Results

Determining the applicability of the panel code to the
swept forward wing was one of the goals of the report. The
wing was chosen because experimental data was expected that
could be used as a data base. From this, the bounds of
validity of the program could be predicted. The parameters
studied in the Wing Performance section were lift, drag,
pitching moment and pressure coefficients. The two con-
figurations used in the initial comparison were the clean
configuration with and without the leading edge glove.
Figures 7 through 18 contain the results of the wing per-
formance analysis.

One of the parameters that this study investigated was
the trim lift of the swept forward wing. The focus of this
section was on the wing alone configuration. The effects
of the canards were also looked at; however, until experi-
mental data is obtained on canard interference effects, the
accuracy of VSAERO's wake interference predictions is
unknown. The parameters studied were lift and pitching
moment coefficients. Figures 19 and 20 present the results
for this section.

Figures 21 through 26 contain the results of the
Spanwise Loading section. This section studied the effects
of leading edge sweep and canard interference effects on

24

the local lift distribution. The Spanwise Loading section also examined the effects of wing twists and the leading edge glove.

The Spanwise Blowing and Boundary Layer Control sections use the wing alone configuration with a 30° trailing edge flap setting to study VSAERO's various options in modeling powered lift. This configuration was placed at an angle of attack of 5. Figures 27 and 28 present the spanwise blowing results. Figures 29 and 30 present the results of the Boundary Layer Control section.

Wing Performance

In Figures 7 and 8 it is shown that VSAERO predicts lift fairly well, up to an angle of attack of 15°. In the linear region of the experimental results, the program slightly underpredicted experimental results. VSAERO also underpredicted experimental results when the leading edge strake, or glove, is attached. The slopes were very accurate, with an error of 3.5% in both cases. Above 15° VSAERO overpredicts and the solution diverged.

The comparison of the drag coefficients was made even though it was realized that the values calculated by VSAERO are questionable. VSAERO's method of calculating drag is to utilize a pressure integration around each section. The results are those of induced drag only with no viscous corrections. Because the wing chosen has only a 5% thickness-to-chord ratio, the CPs calculated by VSAERO at
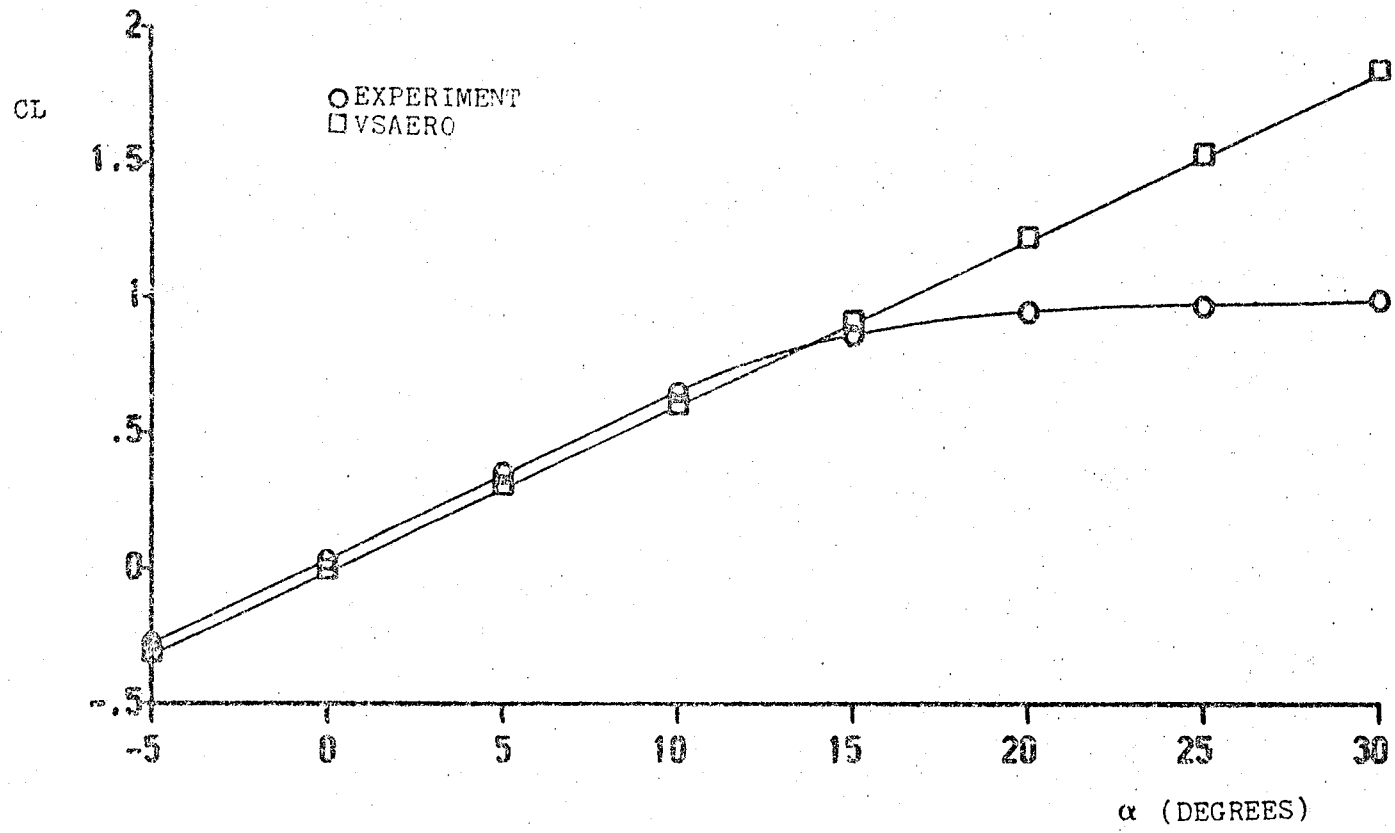
Figure 7
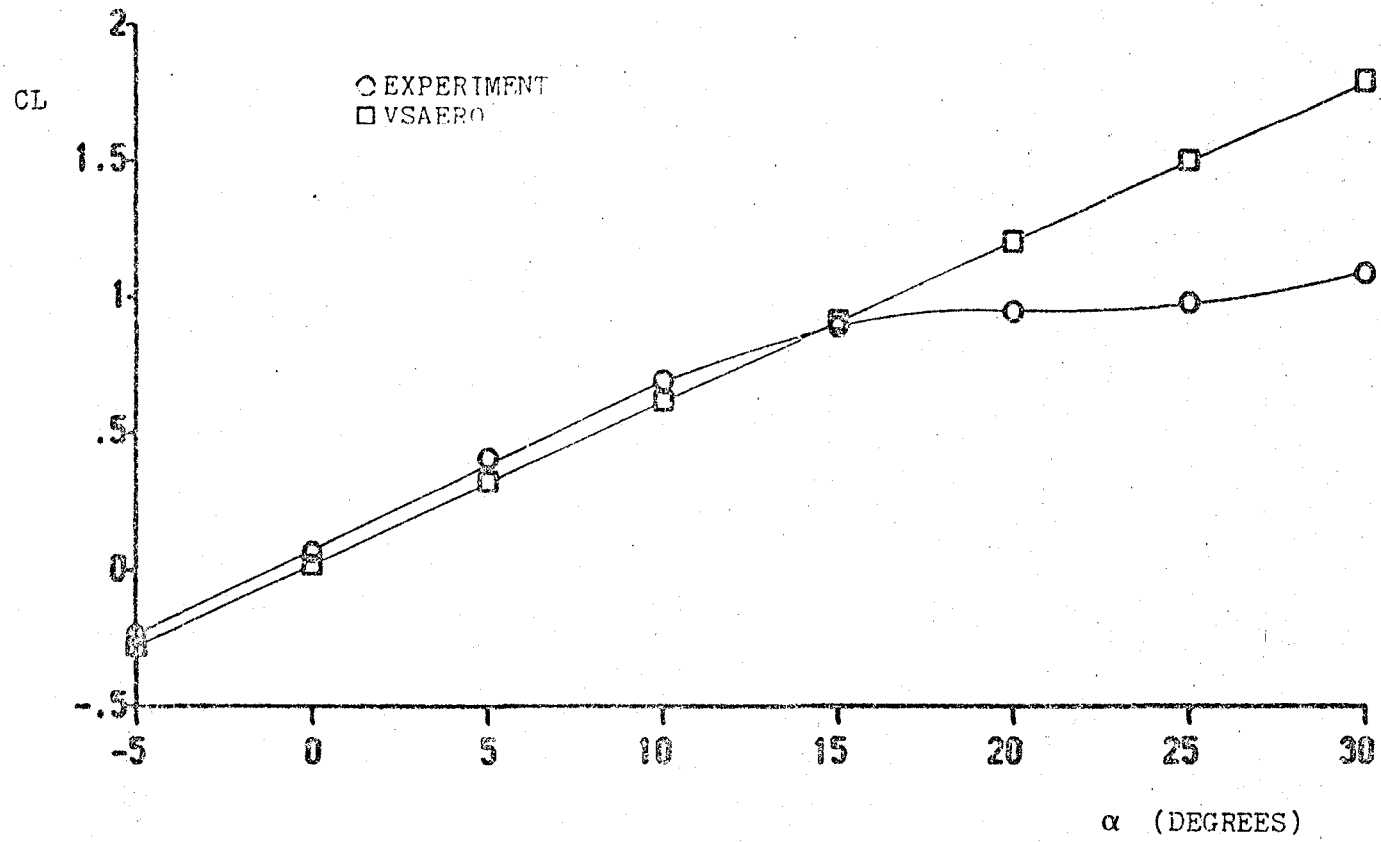
CL vs. α , Wing Only Configuration
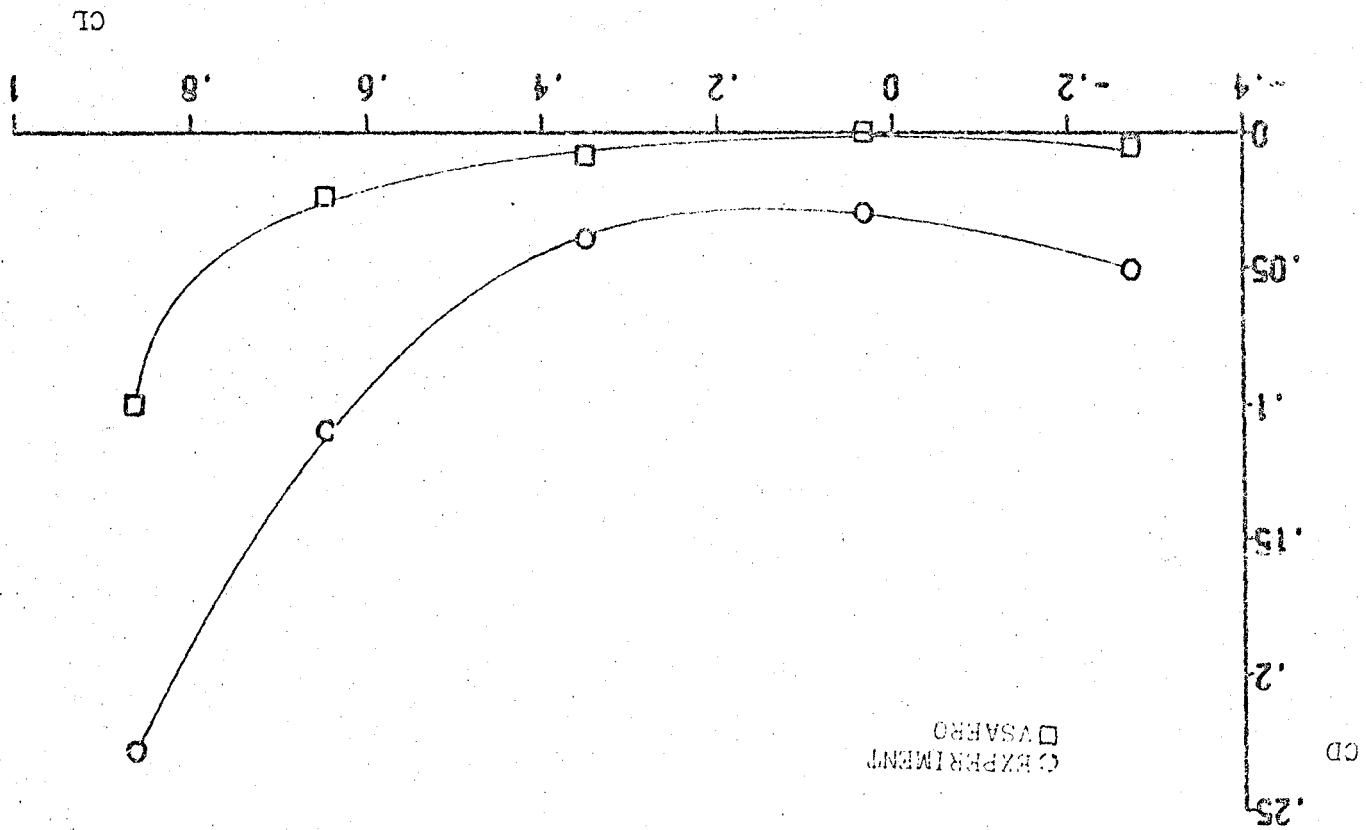
Figure 8

CL vs. α , Wing/Glove Configuration

the leading edge are very high. This causes the CDs to be even more unreliable. When viscous iterations are run, the results are inconsistent and can be as much as an order of magnitude greater than results without the iterations. This was taken into consideration and the values obtained from VSAERO were used only to obtain trends. The results from Figures 9 and 10, with and without the leading edge glove respectively, follow the trends well. However, the values are low.

For pitching moment coefficient comparison, the moment was taken about the X location of the quarter chord of the mean aerodynamic chord at the plane of symmetry. In the 7-by 10-foot wind tunnel test, all forces and moments were measured at the leading edge root without the glove installed. The results from VSAERO for CM were transferred to the leading edge root for comparison with experiment. When the experimental results for the wing alone configuration were linearized, the comparison of the slope with VSAERO was off considerably (see Figure 11). The experimental results for the wing/glove configuration were fairly linear, with the slope differing from VSAERO by 32% (see Figure 12).

The pressure coefficients were compared at three wing stations: 5%, 45% and 90% semispan positions. An angle of attack of 5° was chosen for comparison. With no flap deflections, BLC or spanwise blowing the program compares well with experiment. The program consistently
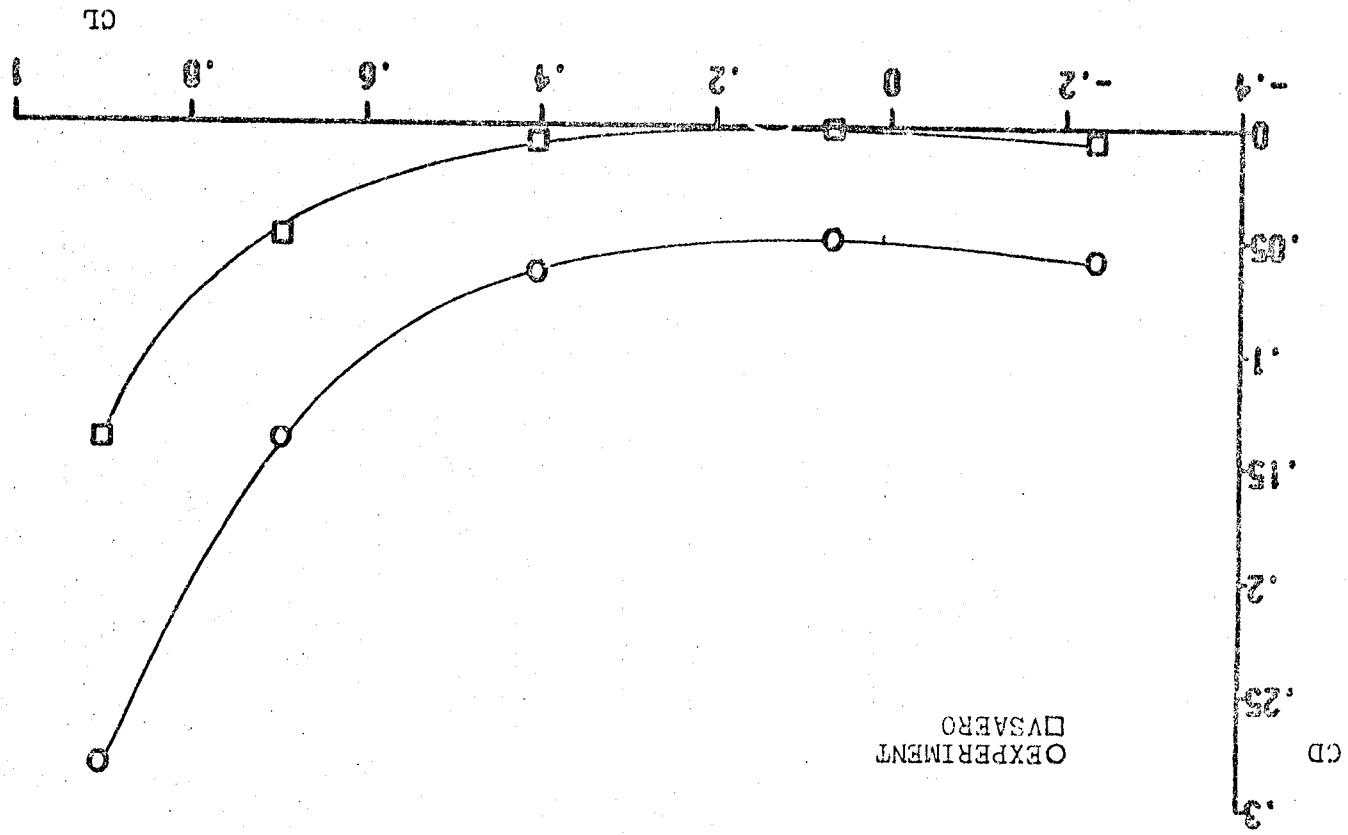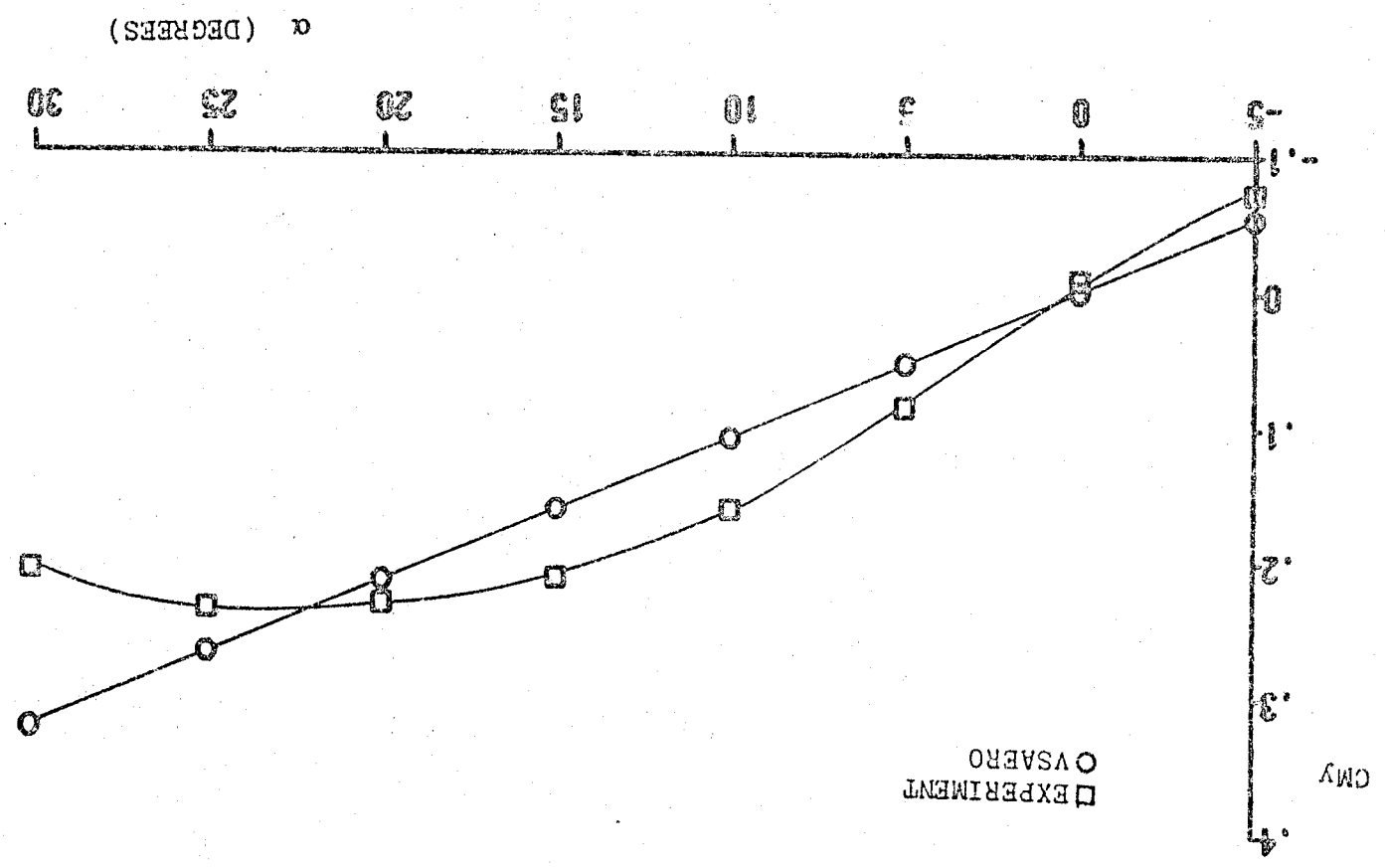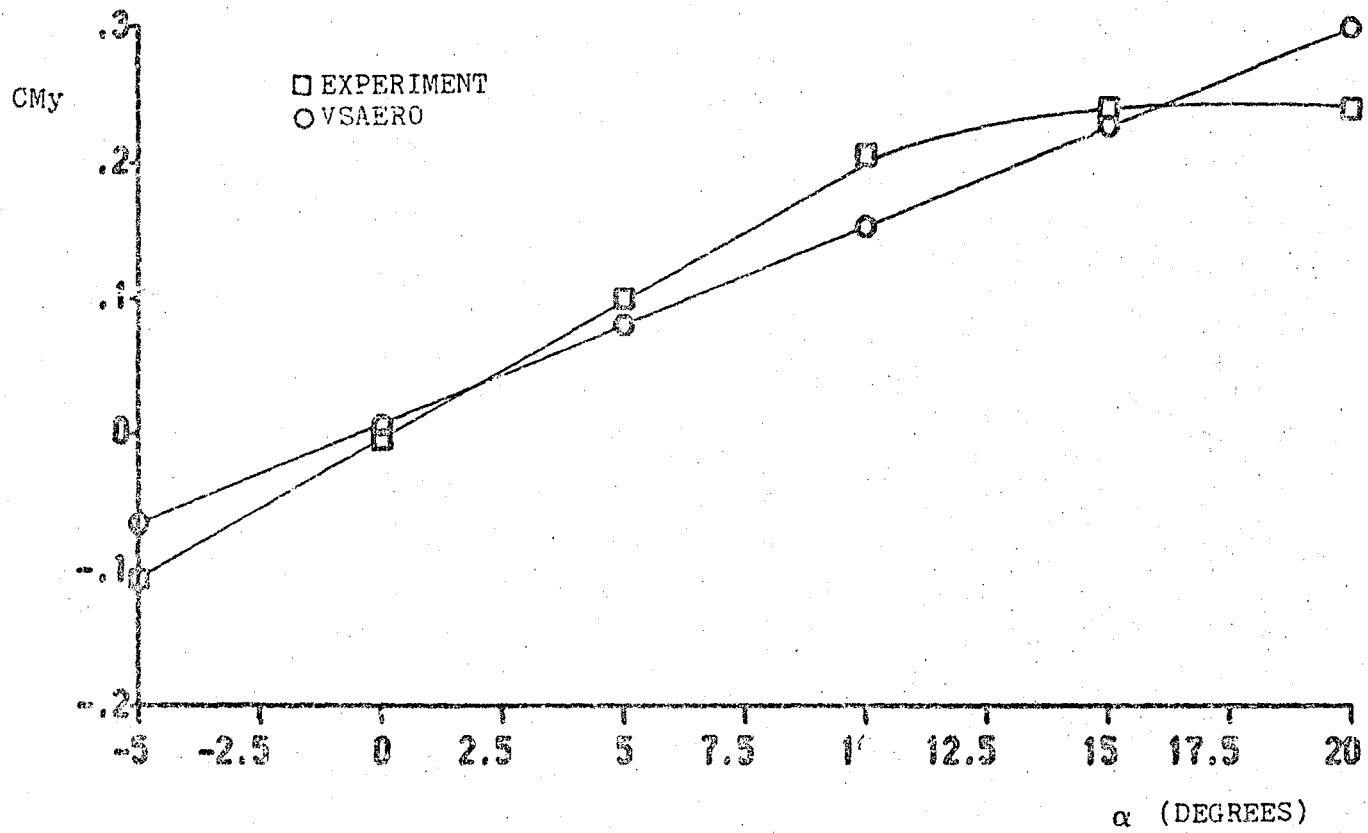
Figure 11

CM vs. α, Wing Only Configuration

31

Figure 12

CM vs. α , Wing/Glove Configuration

underpredicted the negative pressures over the upper surface and the positive pressures on the lower surface. The biggest discrepancy came at the leading edge where VSAERO's values for CP are very high. See Figures 13 through 18 for pressure coefficient comparisons.

The discrepancies in the pressure coefficients may indicate why the pitching moment comparison was off. The pressure coefficients matched fairly closely at the trailing edge of the airfoil, then diverged toward the leading edge. This may have caused the theoretical results to underpredict the positive pitching moment obtained in the experiment. Further study may show that this may again be traced to the sharp leading edge of the airfoil as the cause of the discrepancy. The accuracy of experimental pressure data at the leading edge may also be investigated.

Trim Lift Calculations

The lift at trim of the model was compared with experimental results from the 7- by 10-foot wind tunnel test. From Figures 11 and 12 in the previous section, it can be seen that VSAERO's ability to predict pitching moment is questionable. The experimental results are preliminary and some final corrections may be made. There may be some free stream dynamic pressure variation along the span as well as some additional tunnel corrections.
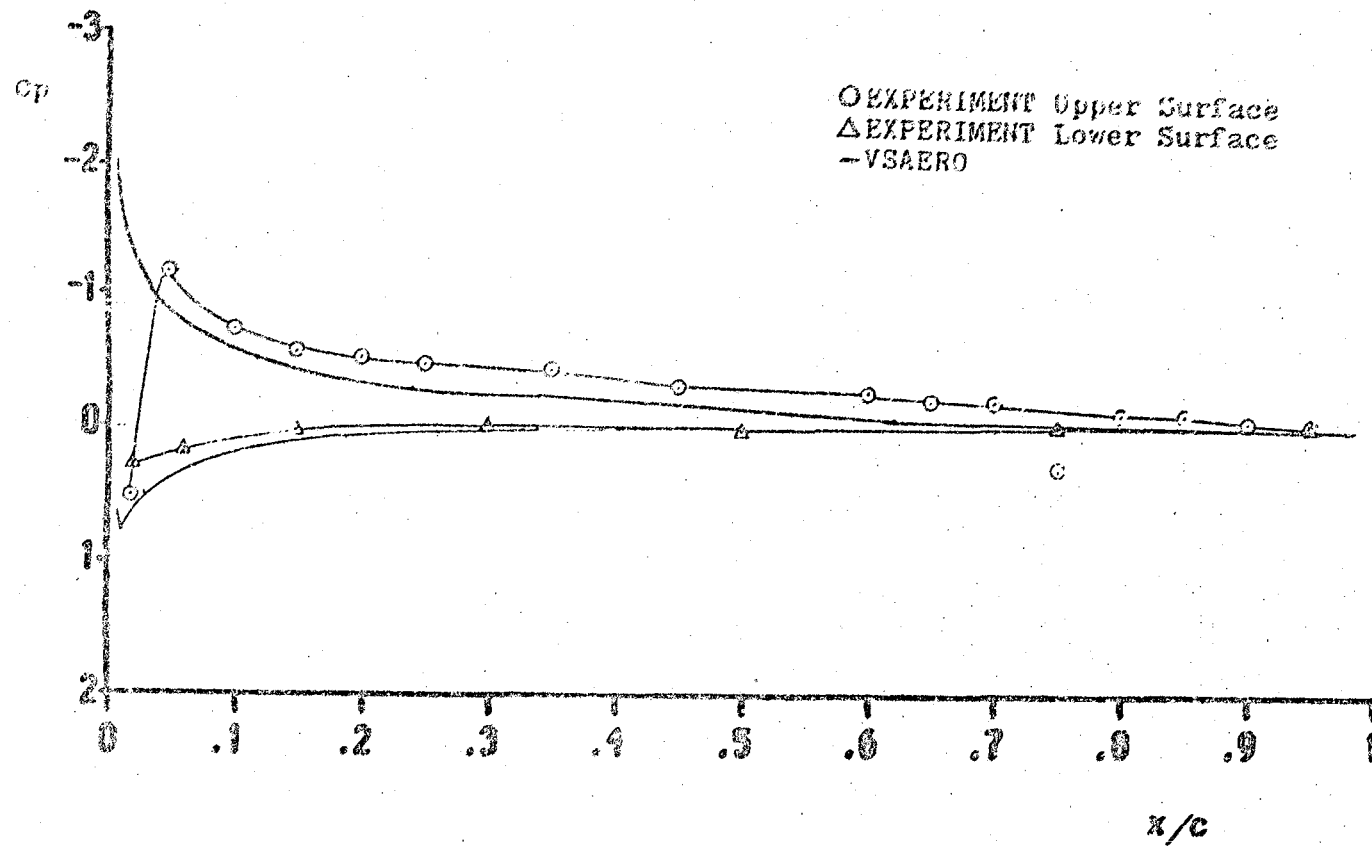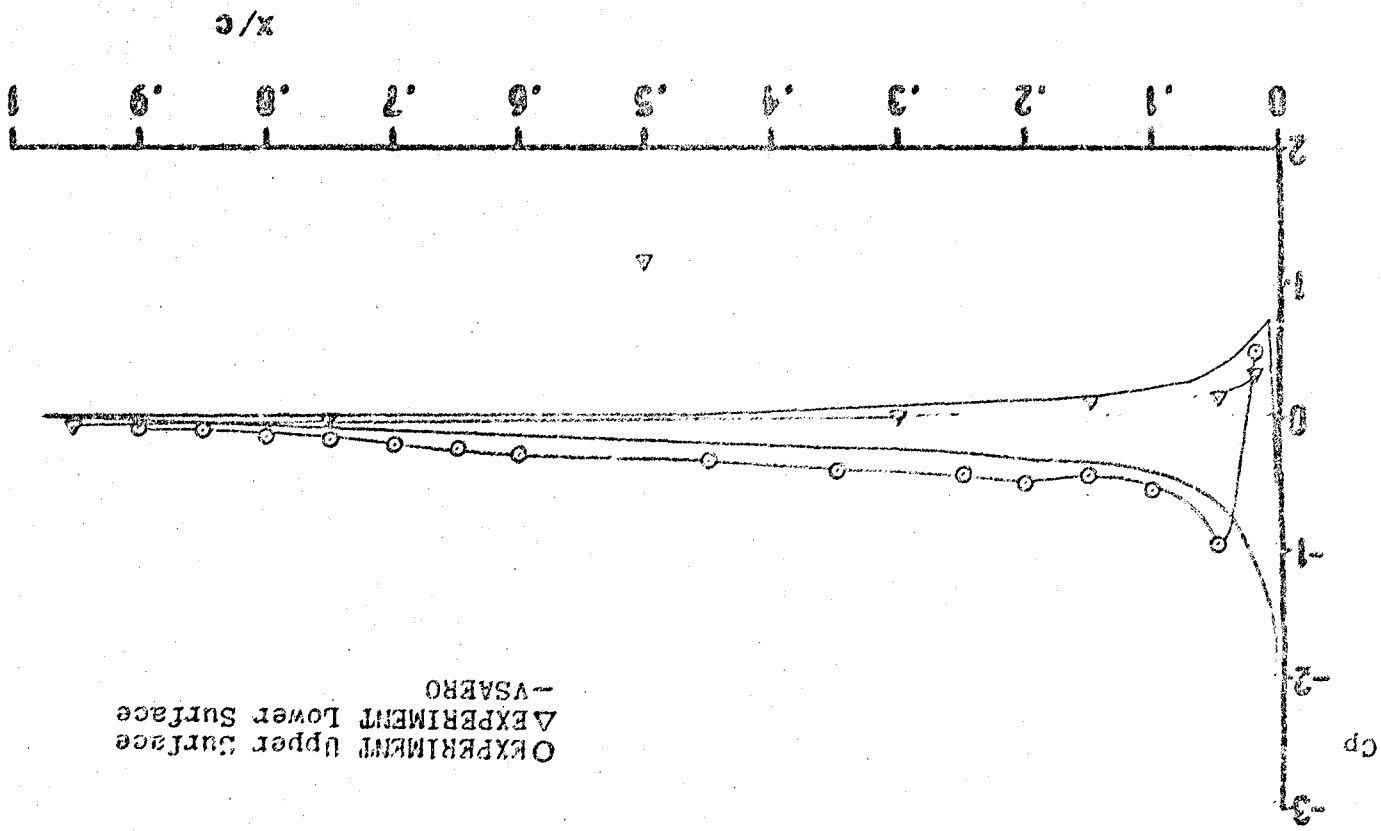
Figure 13

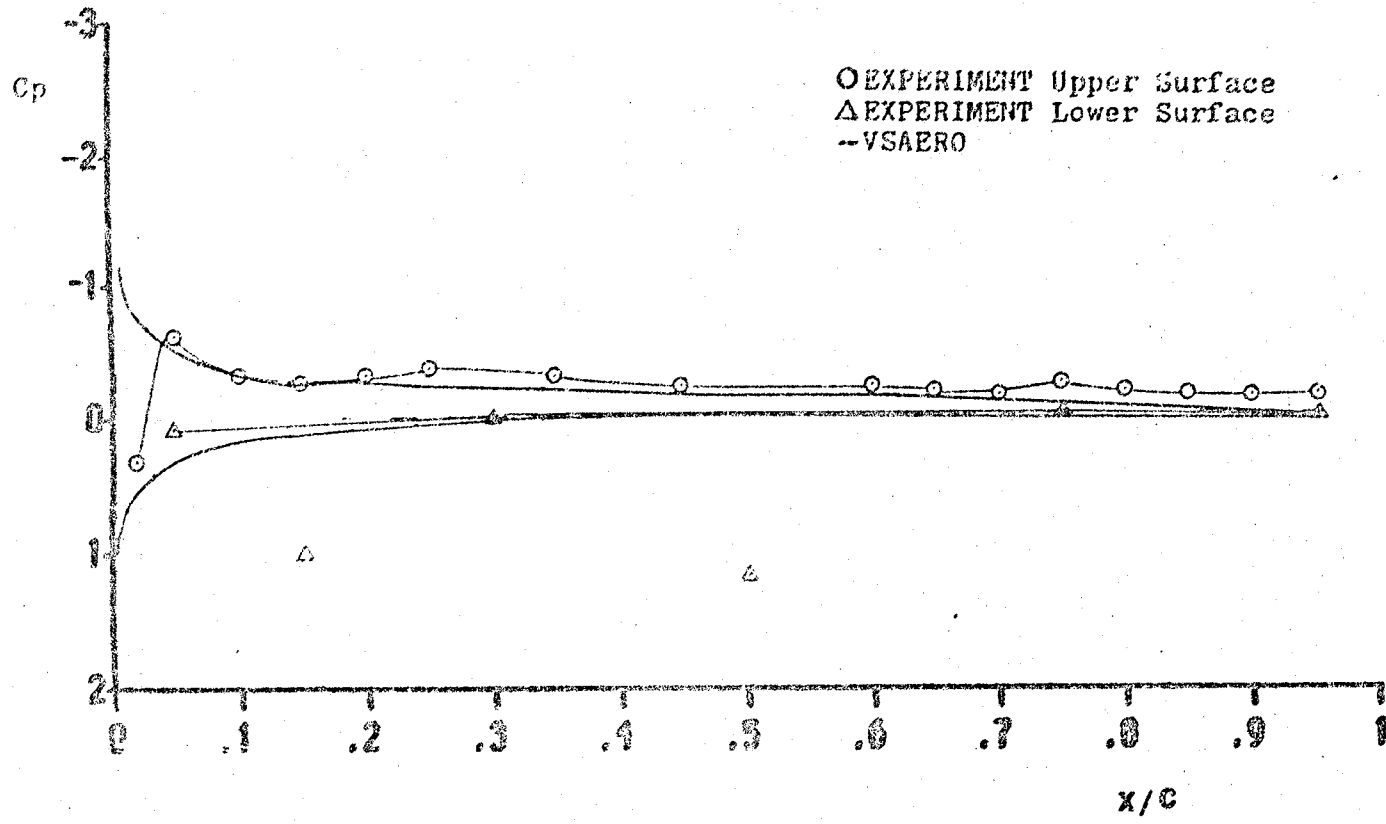CP vs. X/C Wing Only 5° Semispan

Figure 15

CP vs. X/C Wing Only 90° Semispan

Figure 16

Cp vs. X/C Wing/Glove 5° Semispan

X/C

O EXPERIMENT Upper Surface
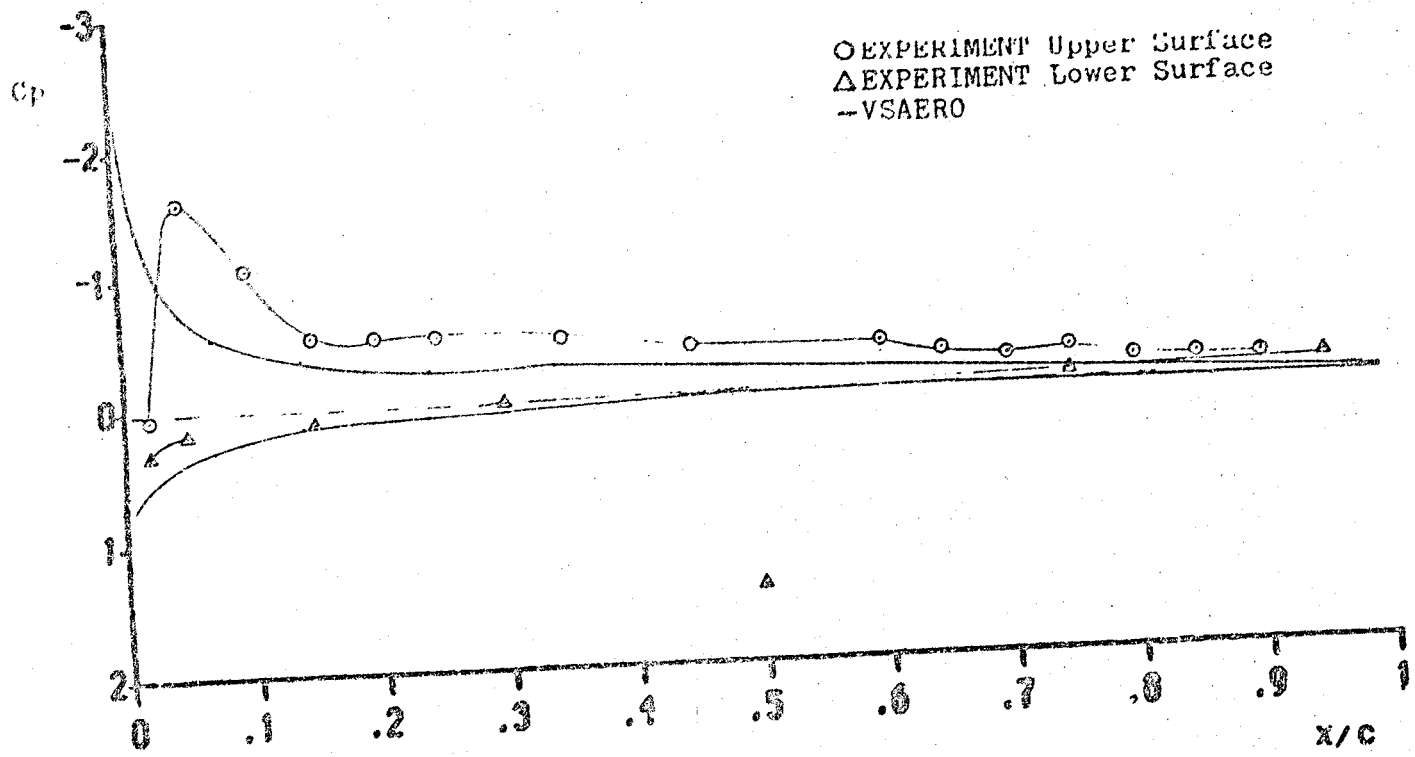△ EXPERIMENT Lower Surface
— VSAERO

Cp
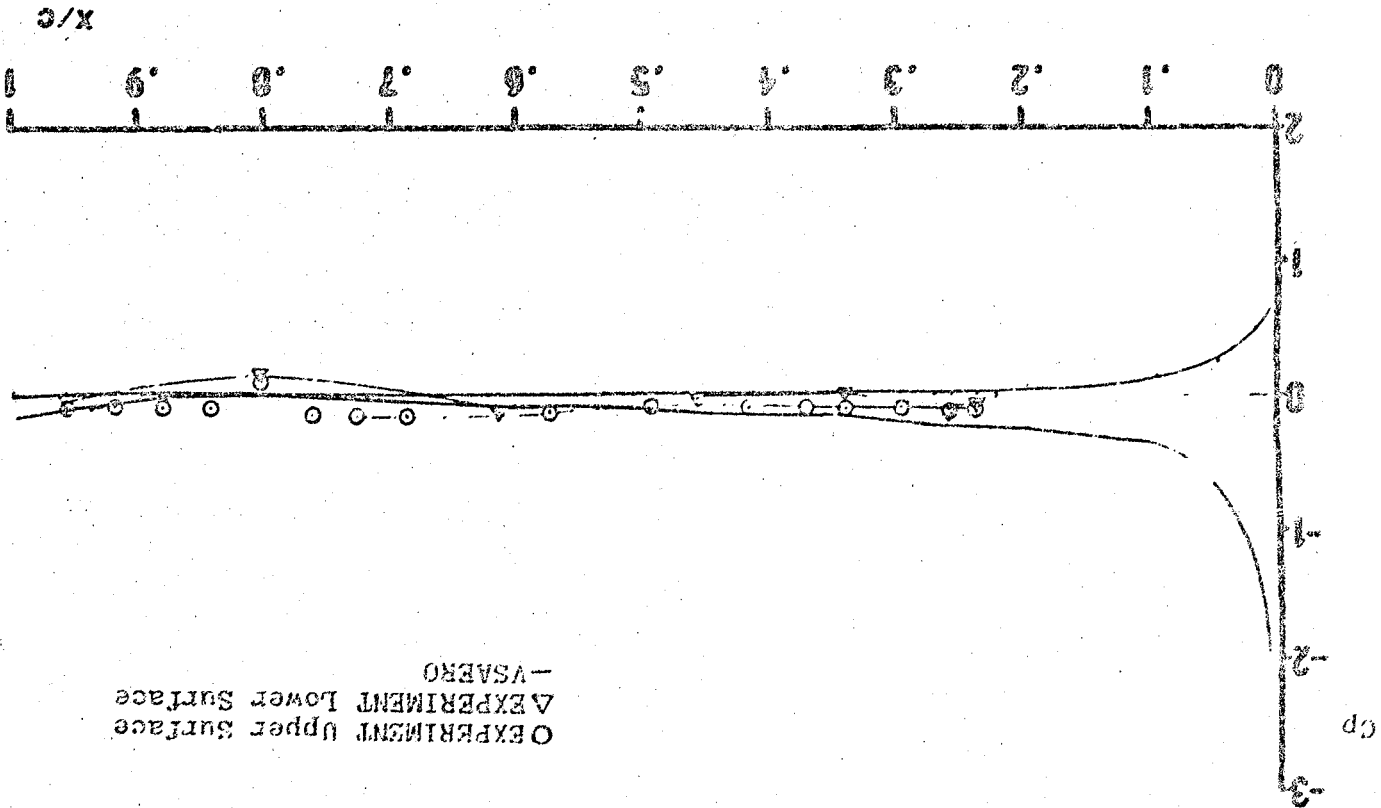
Figure 17

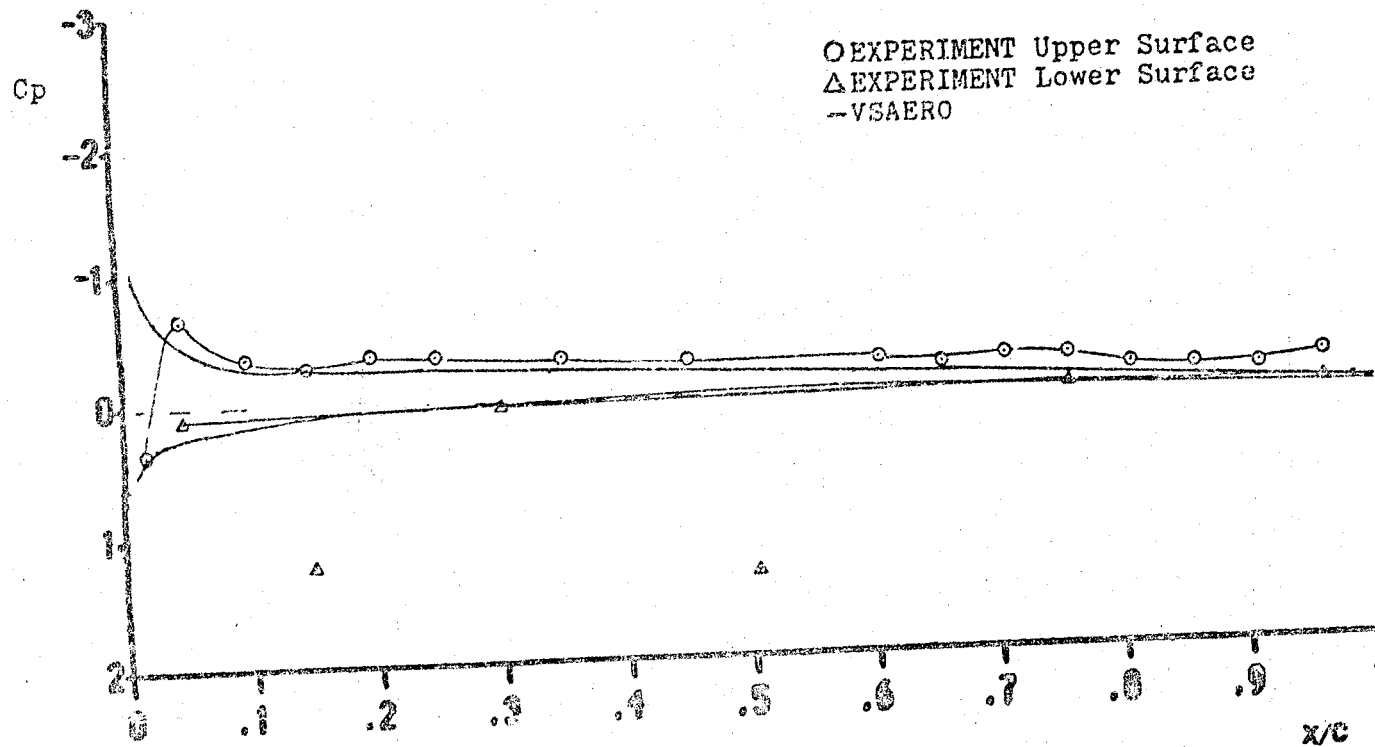CP vs. X/C Wing/Glove 45° Semispan

Figure 18

CP vs. X/C Wing/Glove 90° Semispan

Varying the leading edge sweep will alter the lift
needed to trim the aircraft. With each change in sweep,
the coordinates of the moment center were moved to the new
X position of the mean aerodynamic chord for a $-30°$ sweep.
Figure 19 shows the variation of trim lift with leading
edge sweep. As the leading edge sweep becomes more nega-
tive, the slope decreases. This is expected as the wing
root carries more of the load. For a $-30°$ sweep, the slope
is approximately zero, as it should be for a symmetric wing
with moments taken at the MAC.

In Figure 20, the effects on lift and pitching moment
of Canards 1 and 2 are shown. Both canards effectively
reduce the overall lift produced by the main wing and
increase the slope of the curve. Canard 1, with the larger
relative area, had the greater effect on the results.

Spanwise Loading

With the aft swept wing it is desirable to unload the
tip due to its tip stall characteristics and to achieve a
more elliptical distribution. To achieve this, a wing
twist to reduce tip loading at a given angle of attack or a
"washout" is sometimes employed. With the SFW, the
opposite is true. The wing root needs to be unloaded due
to its root stall characteristics. There are several ways
to unload the root. One is to washout the root with the
proper spanwise twist. Another method is to put a leading
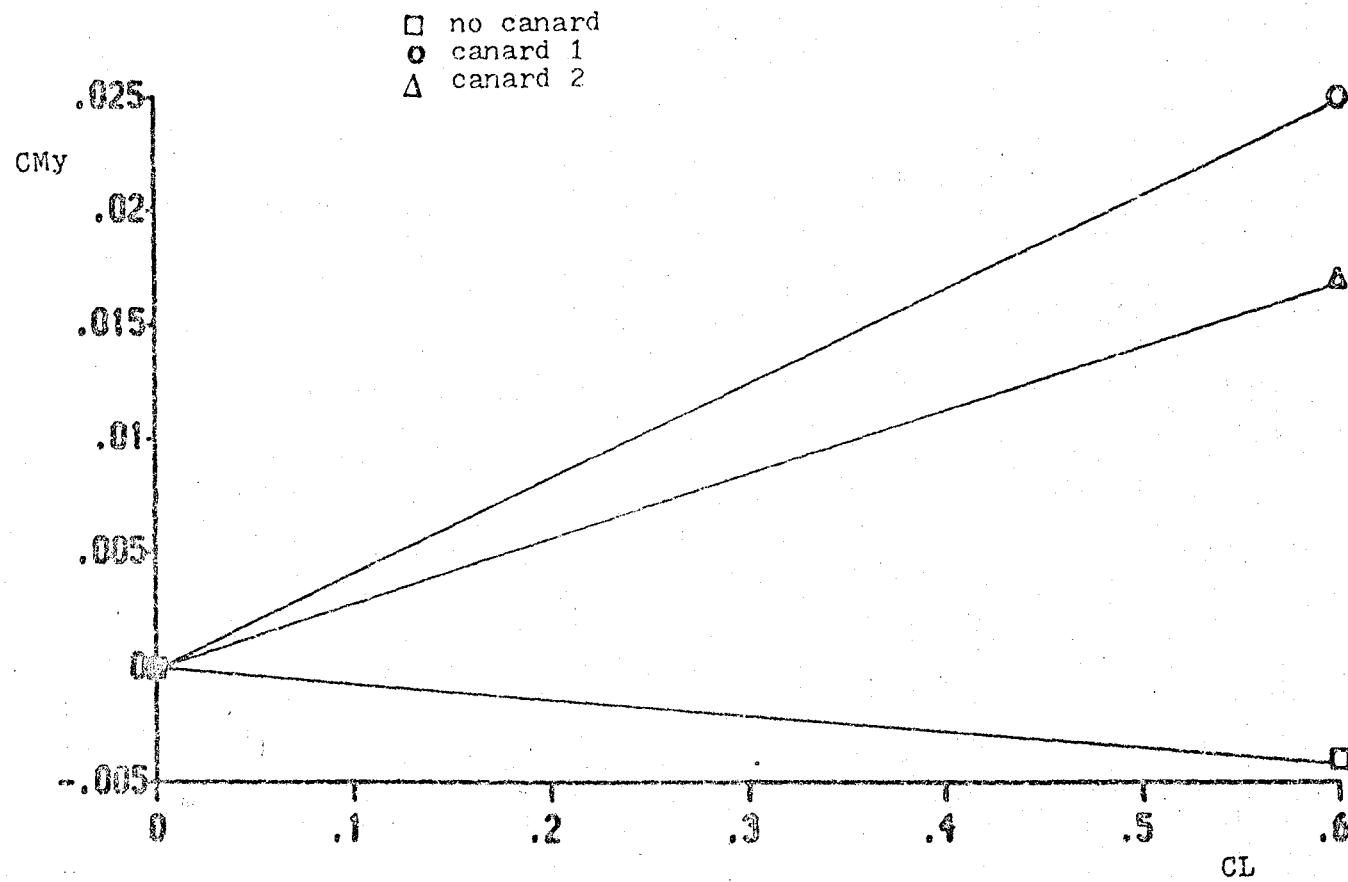edge strake or glove at the wing root. Putting a close
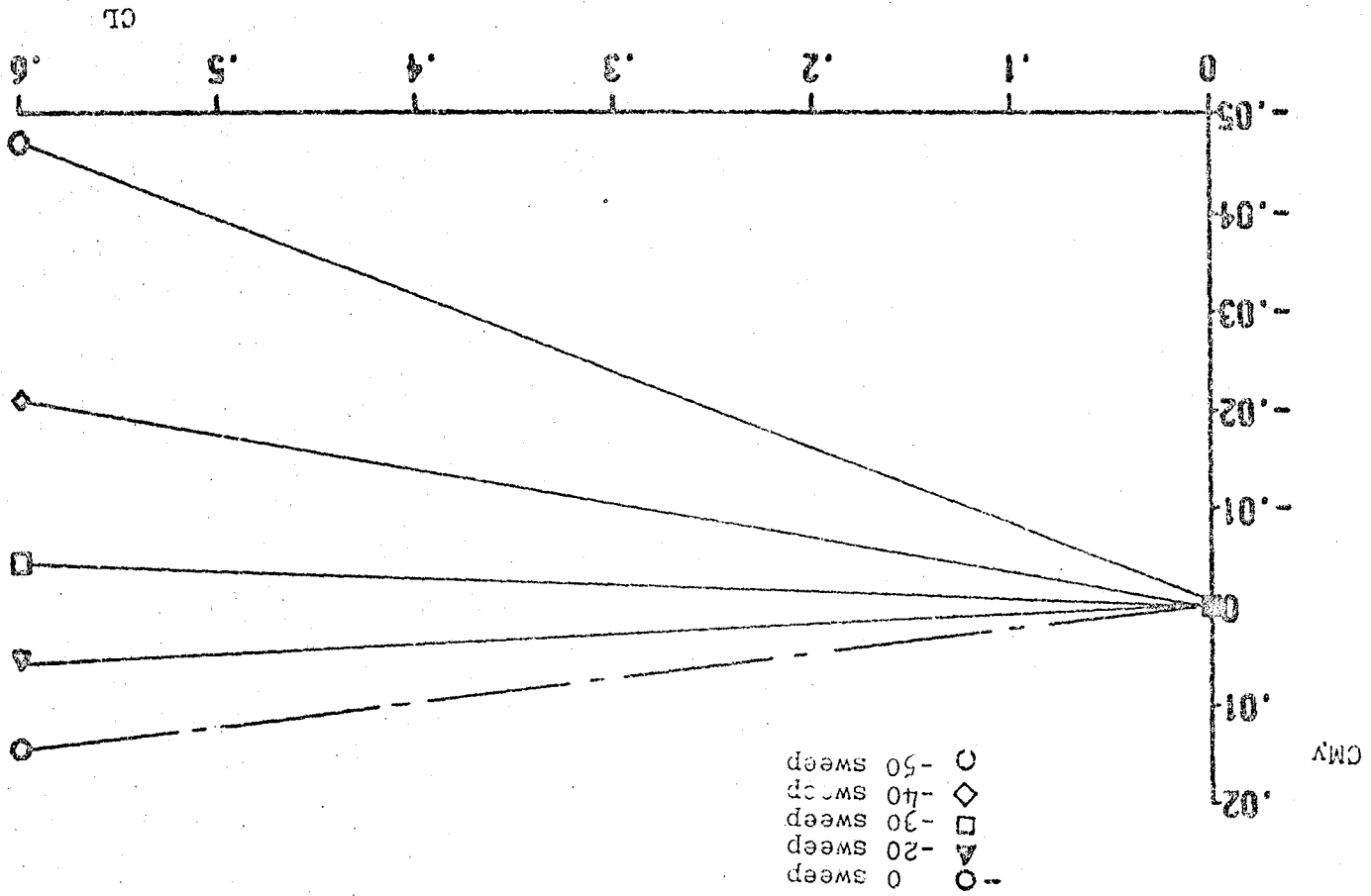
Figure 20

Canard Effects on CM vs. CL

coupled canard into the configuration will also unload the root by reducing the angle of flow into the inboard section. Changing the leading edge sweep is another way of altering the spanwise loading. These four methods of altering the lift distribution were studied and compared to experimental results. Another method of altering the lift distribution is to incorporate a split flap configuration. A split flap configuration was tried; however, the results were not included due to the lack of experimental data for comparison. Figures 21 through 26 show the spanwise variation of lift in terms of $(Cl)(c)/(CL)\ \overline{c}$ at an angle of attack of $5°$.

The effects of the leading edge glove on the clean configuration were to unload the entire wing by about 4% (Figure 21).

The effect of sweep on the lift distribution is shown in Figure 22. The leading edge sweep with the most elliptical distribution came at $0°$, which is to be expected. As the negative sweep was increased, the wing loading became less elliptical.

Several twist variations were computed in order to optimize the lift distribution (see Figure 23). Of the combinations, a root incidence of $-2°$ and a total difference of $2°$ incidence between the root and tip compared best with the elliptical distribution. An elliptical distribution is desirable to lower the induced drag of the airfoil.
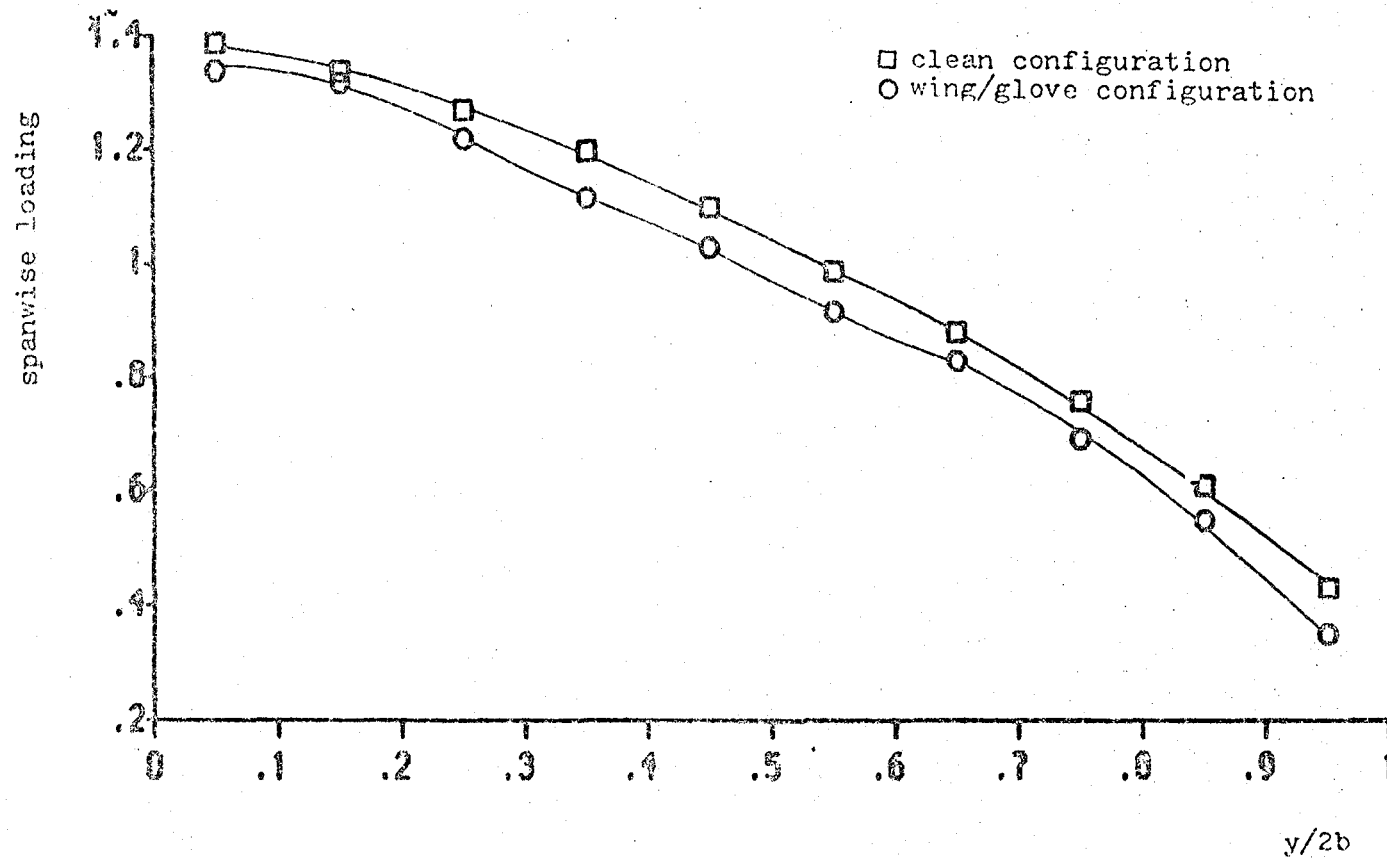
Figure 21

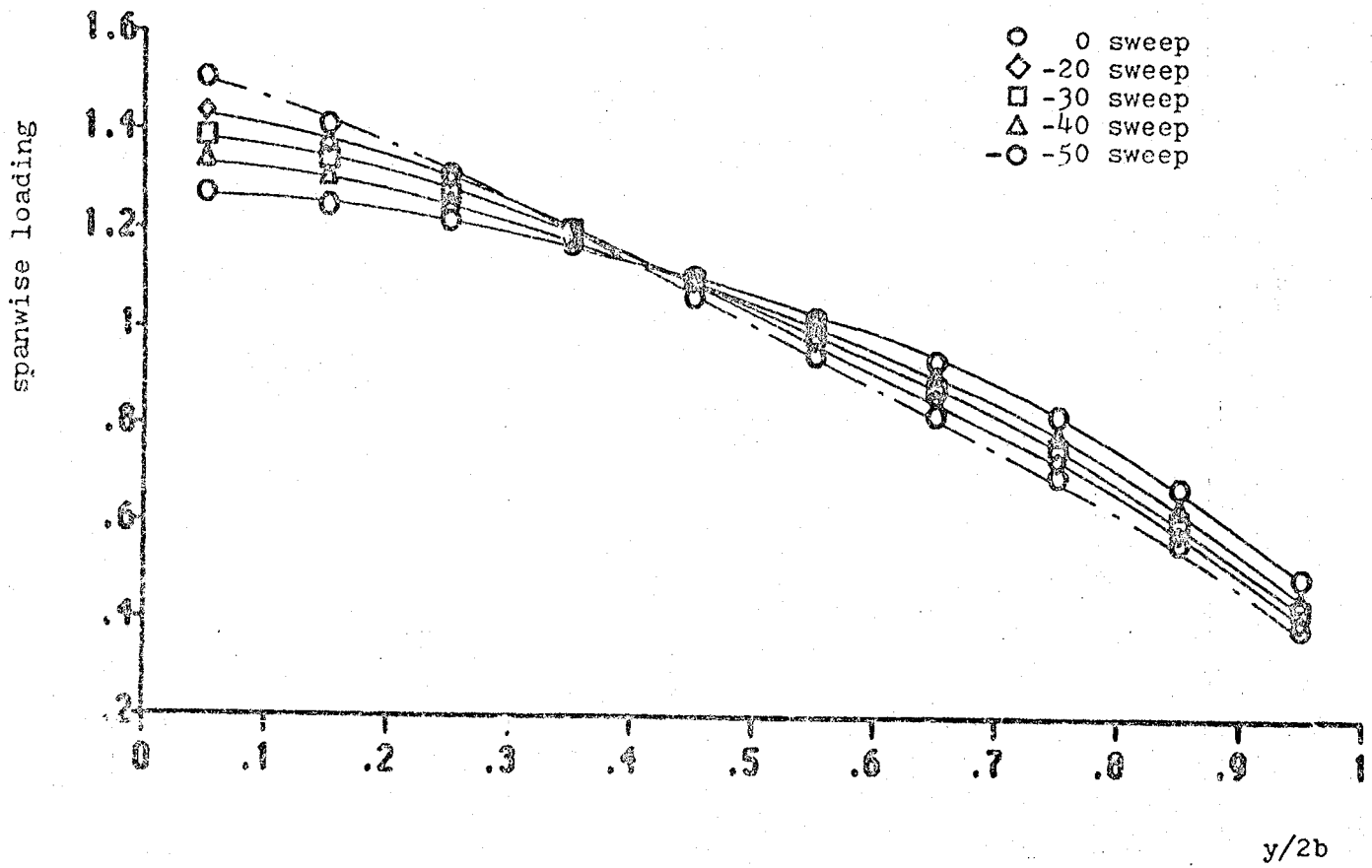Effect of Leading Edge Glove on Spanwise Loading

Figure 22

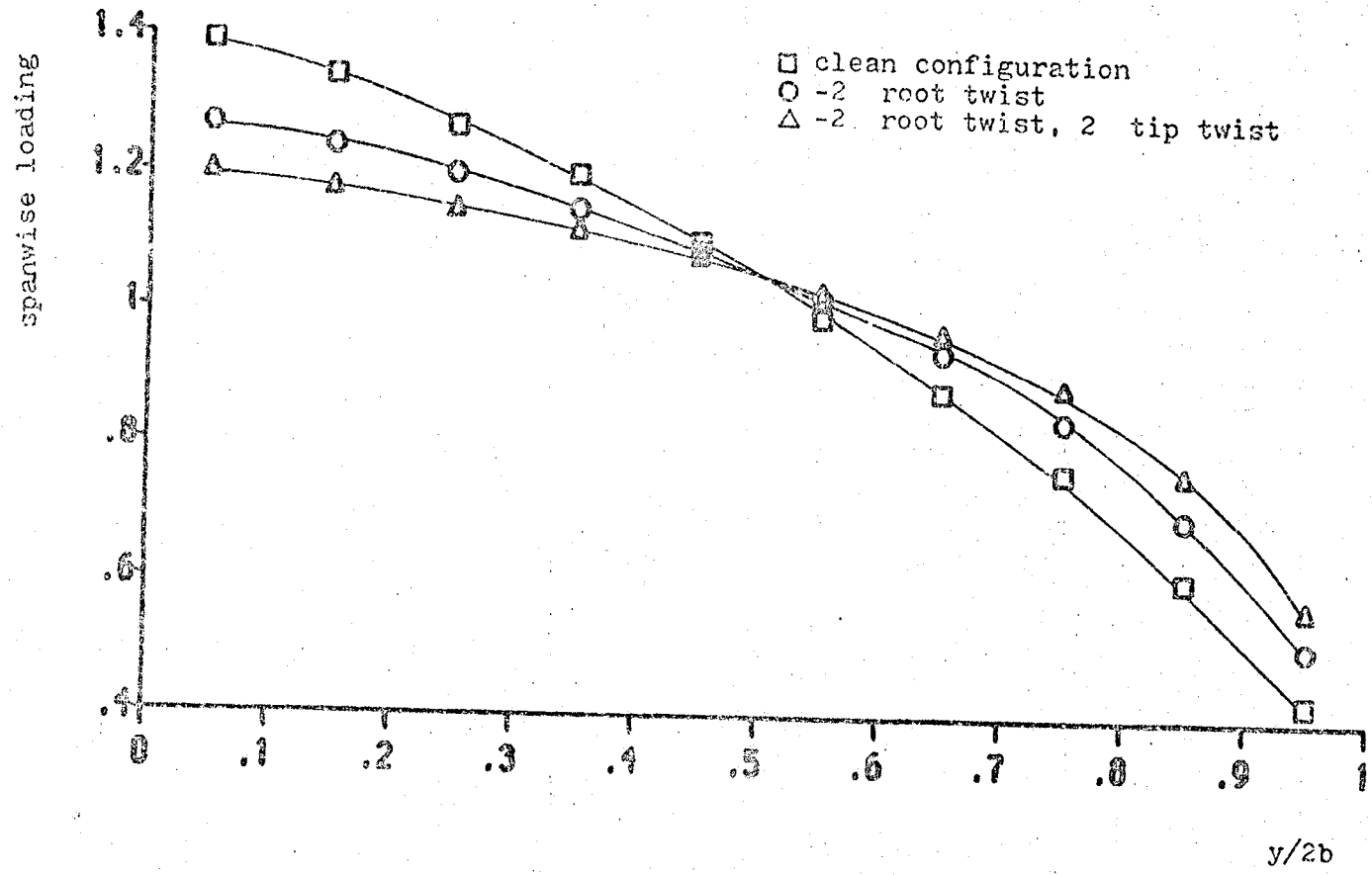$(Cl)(c)/(CL)(\bar{c})$ vs. $y/2b$ for Various Leading Edge Sweeps

Figure 23

Effect of Twist Variations on Spanwise Loading

The effects of canard interference on wing loading were also examined, although no experimental data were available for comparison. The results of VSAERO look encouraging. The curves show what is to be expected with a canard in the configuration. From Figure 24, it can be seen that both canards unload the wing root, while loading up the center and tip of the span. This is the effect of the downwash from the canard caused by the vortex reducing the local angle of attack. With a swept forward wing unloading the root may reduce its root stall characteristics. Of the two canards, the larger canard (Canard 1) unloads the root to a greater extent. When canard location is examined, the effect is greater as the canard is moved closer to the wing (see Figures 25 and 26).

Spanwise Blowing

The options for the BLC flap and the spanwise blowing were to either have a jet wake or to have normal velocities coming from the panels. The following approaches were used in an attempt to model them. All were unsuccessful and the results are not presented.

The jet wake routine failed in modeling the BLC on the trailing edge flap due to program limitations. The program was not designed for this type of application. The program is set up for circular jets not a slot for blowing, causing the result to be unacceptable.
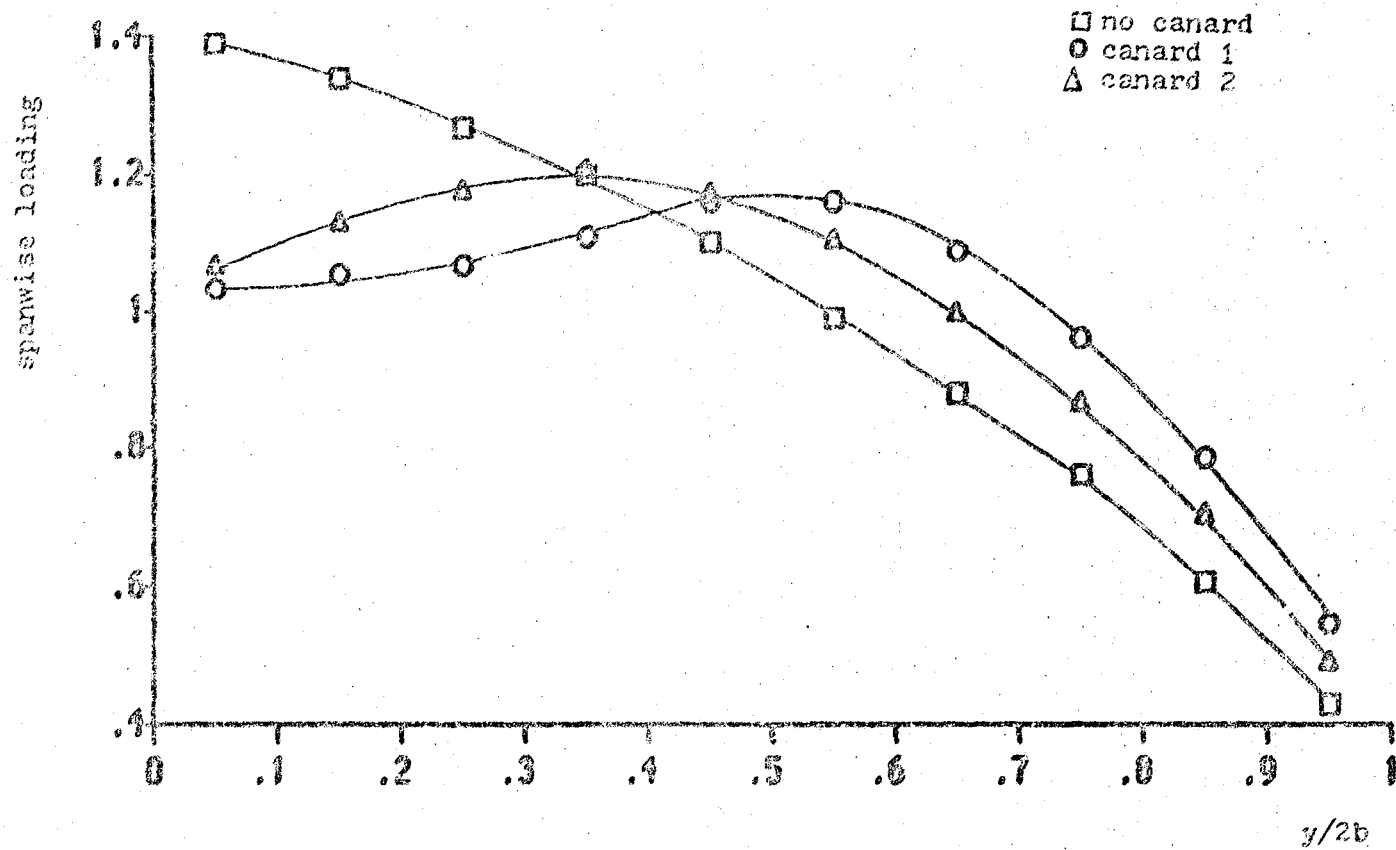
Figure 24

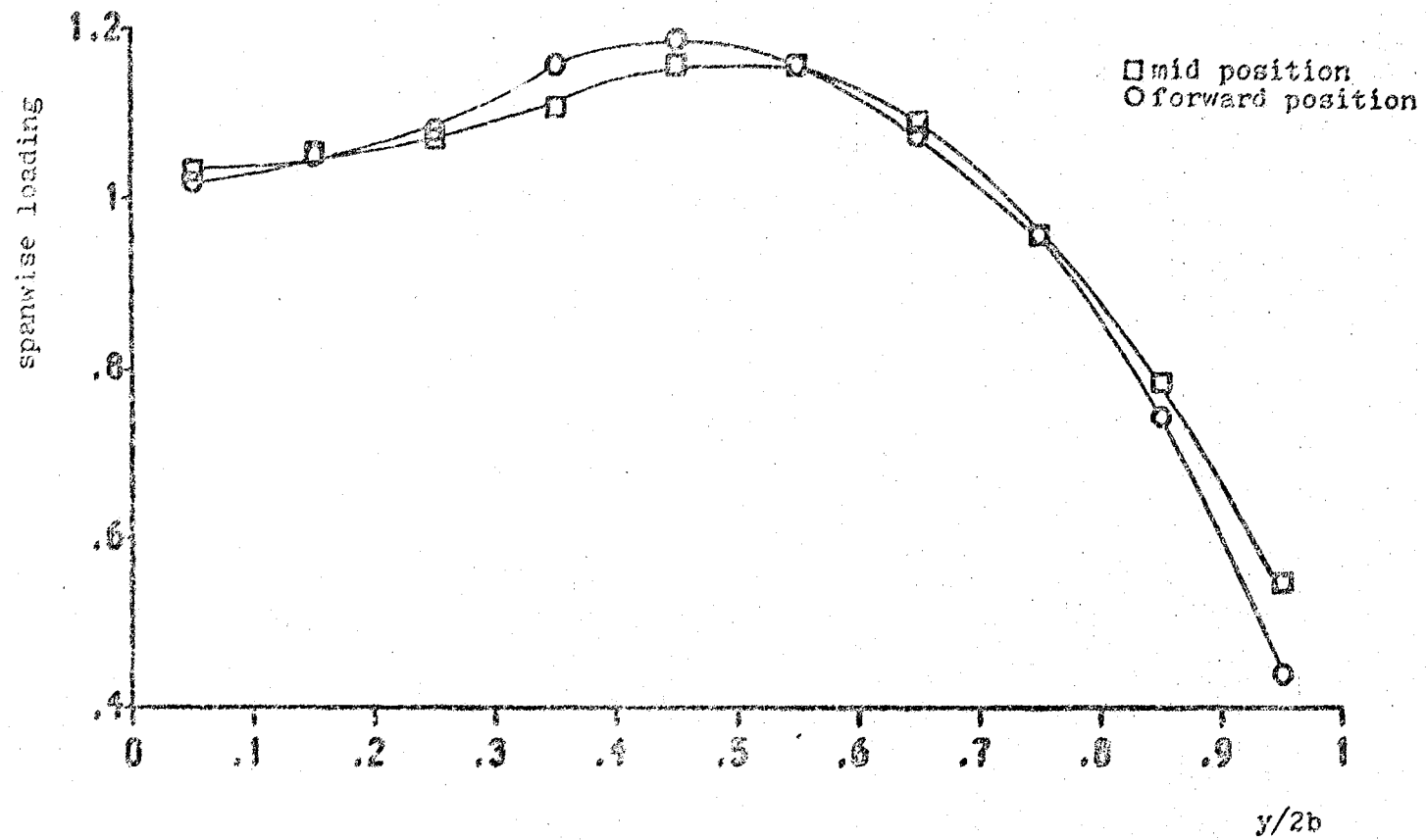Canard Effects on Spanwise Loading
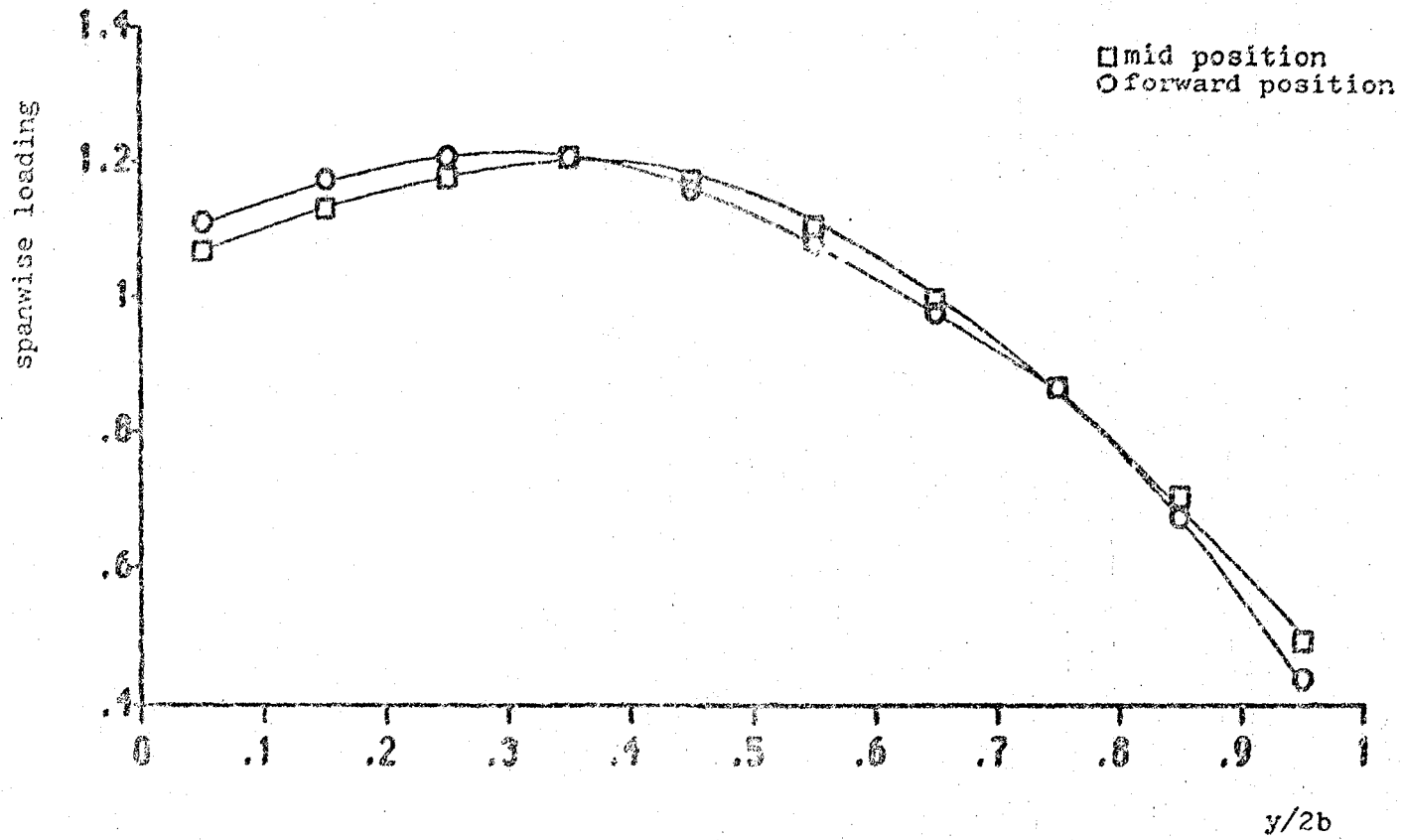
Figure 25

Canard Position Effects for Canard 1

Figure 26
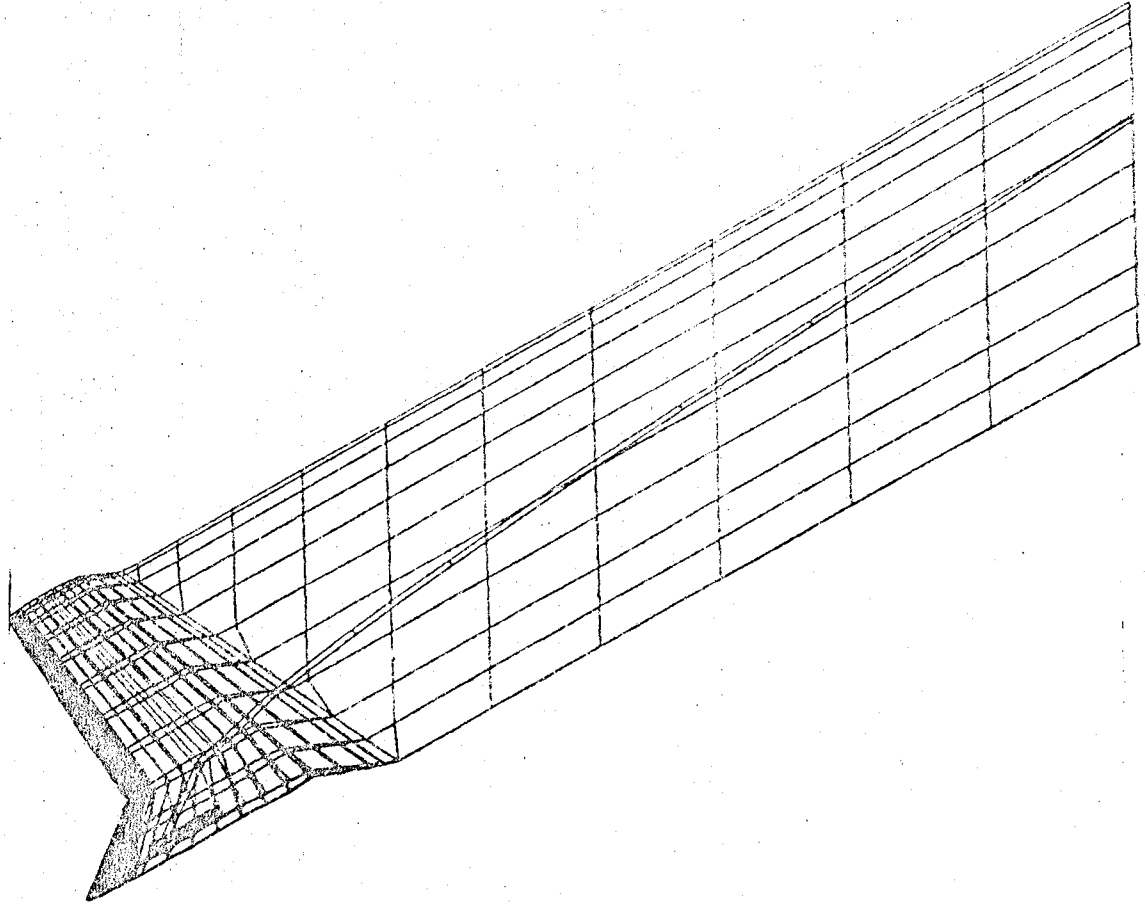
Canard Position Effects for Canard 2

The normal velocity option also proved ineffective for the BLC. This did not model a blown flap but a panel with a very high negative pressure coefficient. This caused the pressure data to be very unstable at the blowing velocities used in the wind tunnel tests.

Three different methods were attempted in modeling the spanwise blowing. The first method was a type three panel or Neumann patch, which was defined at the reflection plane and was given a normal velocity to blow over the wing. Another attempt at spanwise blowing was made with the jet wake module. The jet wake was defined by creating a component above the wing root. The entire geometry was then rotated into the X-Z plane because the jet wake can only be defined to go vertically. Panels were defined along the new reflection plane, the X-Y plane, and the wake was stitched on. The jet wake was then rotated to blow spanwise (See Figure 27). A principal reason for the lack of success for this approach is probably the lack in modeling the entrainment effects of the jet over the wing by the jet wake module.

A final attempt to model the spanwise blowing was to panel a solid body in the empirical trajectory of the jet wake as calculated by VSAERO. Normal velocities were then specified on the leading edge of this solid wake as an attempt to simulate the entrainment. As the solid wake passed over the trailing edge of the flap, it was stopped and a regular wake was stitched on (see Figure 28).
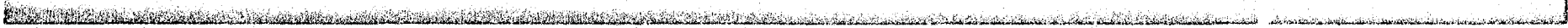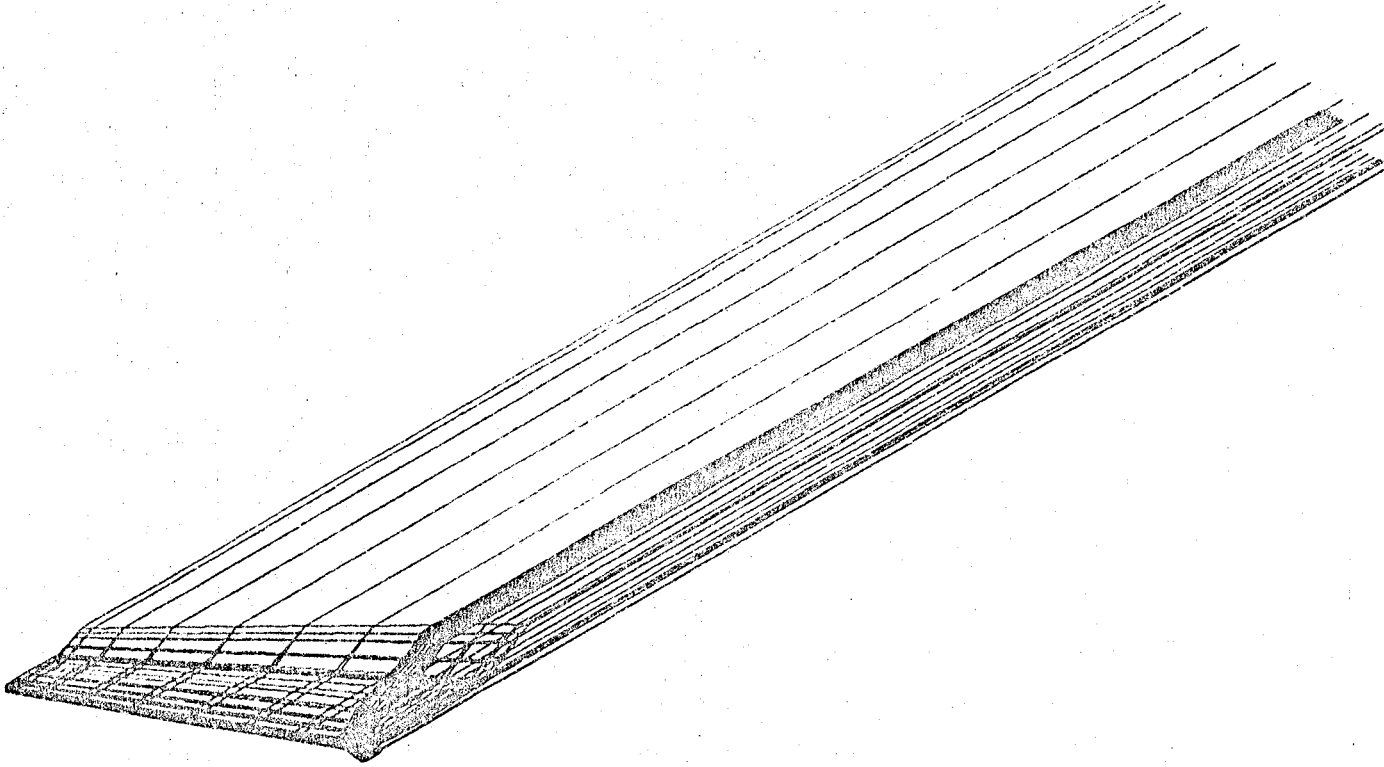
Figure 27

Jet Wake Geometry for Spanwise Blowing

Solid Wake Geometry for Spanwise Blowing

Figure 28

Boundary Layer Control

It was noted, when viscous iterations were abandoned, that the potential flow over the flap might approximate a wing with powered lift devices. A comparison of VSAERO's results with those obtained with BLC in the wind tunnel is shown on Figures 29 and 30. From the figures, it can be seen that the results of the wind tunnel test, which incorporated only BLC, were higher than those obtained from VSAERO. From the nonlinearity of the experimental results, it can be assumed that some jet flap effects may have occurred. The experimenters believe that final calculations of the blowing quantity will put the experimental values of flap blowing in the super circulation range which the existing version of VSAERO does not model without the proper jet entrainment simulation.
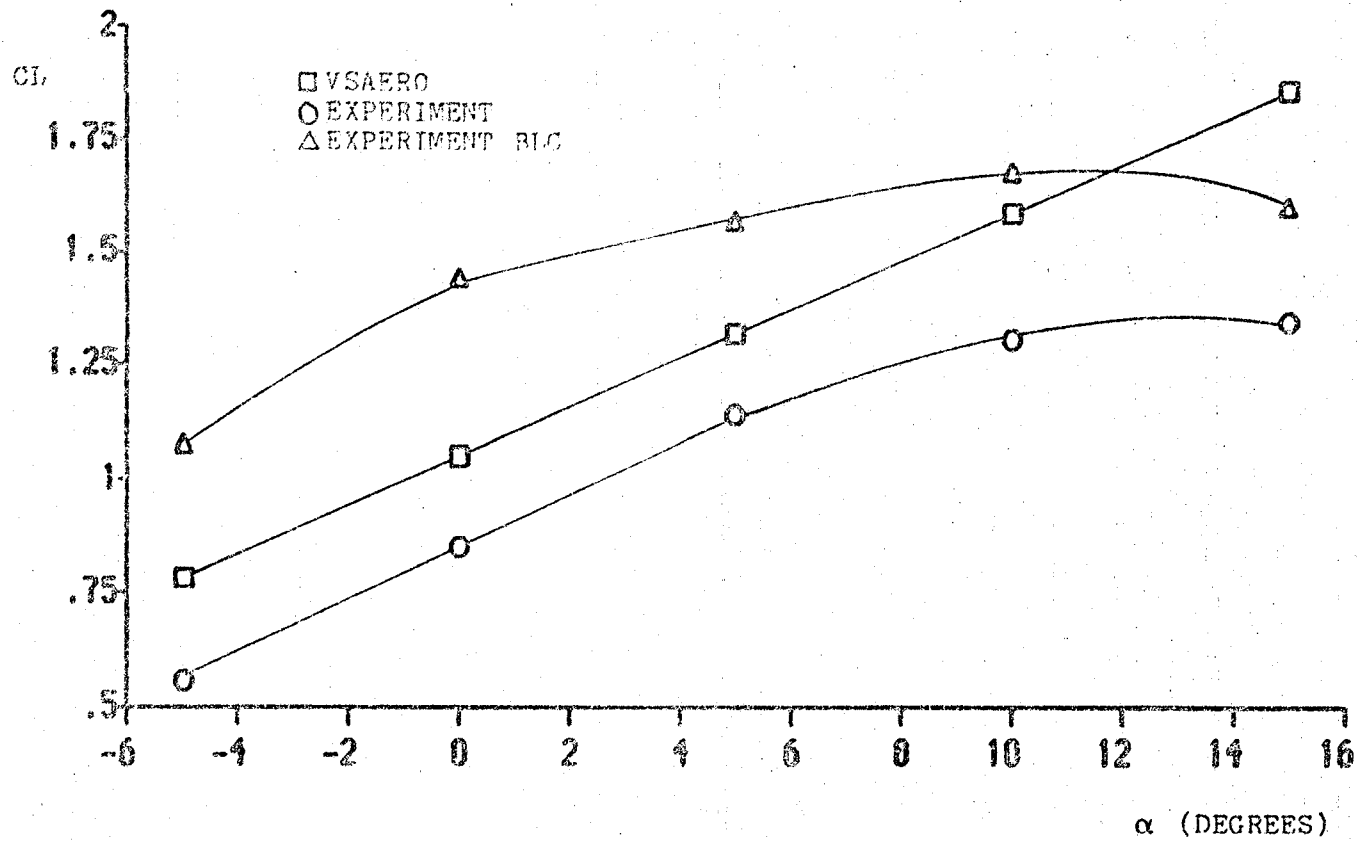
Figure 29

Potential Versus Experimental For Boundary Layer Controlled
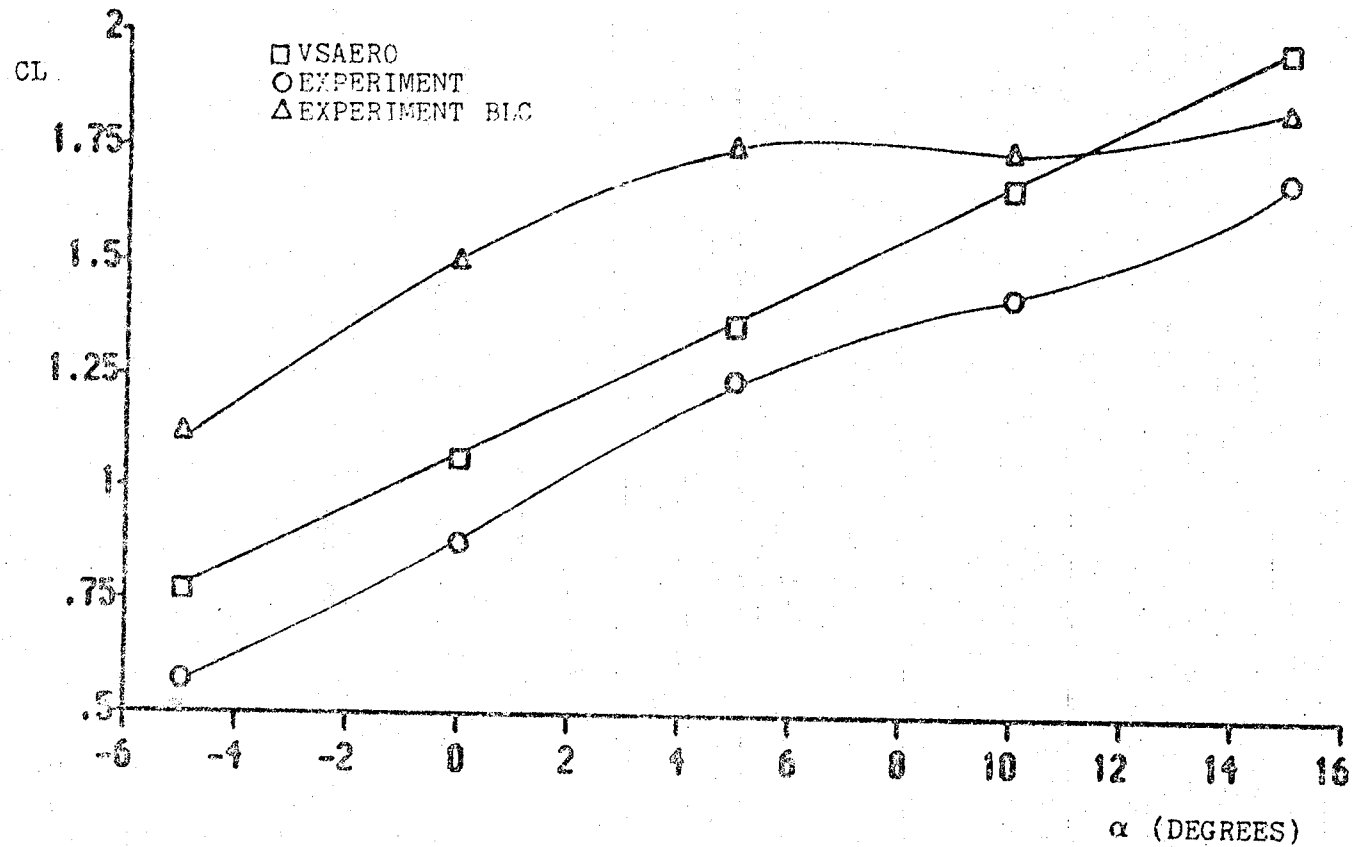Flap Wing Only Trailing Edge Flap 30°

Figure 30

Potential Versus Experimental for Boundary Layer Controlled
Flap Wing/Glove Trailing Edge Flap 30°

CHAPTER 4

Conclusions

After comparing the experimental results of the semi-span model to the theoretical results of VSAERO, several conclusions can be made. The applicability of VSAERO depends on what the user expects to simulate with it. VSAERO will account for most aspects of the configuration in the linear, unseparated flow range. However, once separation becomes a factor, more sophisticated flow modeling must be used and, when possible, installed in the code.

Some limitations of VSAERO were encountered during this investigation. The most restrictive limitation was the inability of VSAERO to handle the sharp leading edge of the airfoil. Because of this, it was not possible to run boundary layer calculations and viscous iterations. It limited the use of the experimental data to angles of attack below 15° or, otherwise, test conditions that were shown to produce little or no separated areas on the model. For the same reason, it was also not possible to calculate accurate streamlines and separation lines.

The lack of a sufficient model for the boundary layer control flap and the spanwise blowing was another limitation. In addition, the restriction in attitude and the lack of experimental results limited the study of close coupled canard induced effects.

When compared to experiment, VSAERO was accurate in predicting lift and pressure coefficients at the lower angles of attack. Up to 15°, VSAERO predicted the lift curve slope to within 3.5%. The pressure coefficients compared favorably with those of experiment, with the trends following closely. Pitching moment coefficients did not match as well as was hoped. This might be traced to the sharpness of the leading edge. The drag calculations are only capable of giving the user general trends and restricted the study of the overall drag predictions.

The results of the trim lift investigation are questionable. VSAERO's ability to predict the pitching moment of the experimental swept forward wing was not good. However, the trends may be assumed to be correct. The effects of the leading edge sweep and the canards were also examined, with encouraging results.

The results from the investigation of spanwise loading were favorable. The program showed the trends one would expect by changing wing sweeps, leading edge strake and wing twists. The canard induced effects also followed what would be expected, with the wing root being unloaded.

An attempt at modeling the spanwise blowing and boundary layer control was also made, although with little success. At the time, the options available for modeling the powered lift devices were limited. There is an effort now at NASA to update VSAERO to simulate the effects of power induced aerodynamics.

APPENDIX

59

Developing a method to model the separation of the trailing edge flap was important if a correct representation of the flap performance was to be obtained. If the separation is not modeled, VSAERO will assume potential flow over the flap and the resulting answer will be optimistic. For the development of the wake, an angle of attack of five degrees and a trailing edge flap deflection of thirty degrees were chosen.

Initially, a jet wake was stitched on running clockwise enclosing the flap. This puts the inside of the jet wake on the flap itself and the freestream as the outside. With a jet wake, velocities on the inner and outer surface of the wake have to be specified. No wake iterations were specified until a good match could be made between the specified inner and outer velocities and the resulting velocities calculated by VSAERO.

The initial results were not encouraging and a better definition of the wake path was specified. The wake was paneled to go parallel with the streamwise axis off the flap hinge line and trailing edge. The wake lines off the root and tip were then splayed to fill the gap. This definition of the wake trajectory became the standard initial geometry.

Although the results of the jet wake model were improved by the new wake trajectory, the pressure coefficients on the flap crossed over to where the pressure on the lower surface was less than on the upper surface.

Several different velocity ratios were tried between the inner and outer surface of the wake, but a satisfactory answer could not be achieved. It was speculated that to get a good answer, the velocity ratio of each wake column would have to be specified. The time and work needed to do that was prohibitive.

The next wake type tried was the Type 3 wake or the separated wake. When the initial splayed wake was stitched on, the results from this type of wake were considerably lower than measured and previous VSAERO calculations. The pressure coefficient crossover on the flap was also generated using this configuration. The next wake pattern tried with a Type 3 wake was two separate wakes running spanwise, with no splayed wakes at the root or tip. The results of this were basically the same, with an underestimation of the true lift. Relaxing the wake had little effect on the result.

A regular Type 1 wake was then stitched on in the initial splayed wake configuration and in the double wake spanwise configuration. The Type 1 wake was consistently high. The pressure coefficient crossover was also present.

With the three wake types tried, a satisfactory answer was not obtained. A combination of wake types was modeled next. A Type 3 separated wake was stitched on the hinge line and a regular wake was stitched on the trailing edge at the deflection angle. This model gave good results, with no pressure coefficient crossover. With this model,

viscous iterations were specified but proved to be inaccurate. Since the viscous iterations proved to be inaccurate, no viscous calculations were done and the wake was allowed to relax.

The combination of Types 1 and 3 wakes was chosen as the best way to model the separated wake based on these results.

End of Document